CHALMERS
UNIVERSITY OF TECHNOLOGY

A novel approach to the design of rear airfoil pylons on high performance car

Master's thesis in Automotive Engineering

Oskar Hellsten
Oskar Pettersson

Department of Mechanics and Maritime Sciences
CHALMERS UNIVERSITY OF TECHNOLOGY
Gothenburg, Sweden 2020

Master's thesis 2020:37

A novel approach to the design of rear airfoil pylons on high performance cars

Oskar Hellsten
Oskar Pettersson

CHALMERS
UNIVERSITY OF TECHNOLOGY

Department of Mechanics and Maritime Sciences
Division of Vehicle Engineering and Autonomous Systems
Chalmers University of Technology
Gothenburg, Sweden 2020

A novel approach to the design of rear airfoil pylons on high performance cars
Oskar Hellsten
Oskar Pettersson

Supervisor: Magnus Urquhart, Department of Mechanics and Maritime Sciences
Supervisor: Ugo Riccio, Lamborghini Automobili S.p.A
Supervisor: Vincenzo Sepe, Lamborghini Automobili S.p.A
Examiner: Lennart Löfdahl, Department of Mechanics and Maritime Sciences

Master's Thesis 2020:37
Department of Mechanics and Maritime Sciences
Division of Vehicle Engineering and Autonomous Systems
Chalmers University of Technology
SE-412 96 Gothenburg
Telephone +46 31 772 1000

Cover: Visualization of the flow going over the car towards the wing and pylon.

Printed by Chalmers Reproservice
Gothenburg, Sweden 2020

A novel approach to the design of rear airfoil pylons on high performance cars
Masters's Thesis in Automotive Engineering
Oskar Hellsten & Oskar Pettersson
Department of Mechanics and Maritime Sciences Division of Vehicle Engineering and Autonomous Systems Chalmers University of Technology

Abstract

The continuous improvement of every aspect of the car is what makes Lamborghini one of the leading super sports car manufacturers of the world. One of the areas that is to be investigated is the pylon, which attaches the rear wing to the car body. There are two main aerodynamic components of the pylon that could help to increase the performance of the car; the reduction of drag on the pylon and the ability to create a lateral force that could help while the car is cornering. This thesis aims to make an initial aerodynamic investigation of the shape of the airfoil that makes up the pylon to see what benefits that could be gained.

At the start of the thesis, it was concluded that the pylon should be symmetric to be able to handle oncoming wind from different directions and that the investigated wind attack angle should span from 0 deg to 15 deg with a focus on the 0 deg to 5 deg region. A base airfoil shape was developed using an optimization method and CFD to test many different shapes efficiently and find the best one out of those. With the base shape set, different geometrical features were added to the base to see if that could improve the airfoil performance. One of the concepts had slots that went through the base airfoil, another one was a double airfoil that consists of two smaller sections. The same optimization method was used for the slots respectively the shape of the two airfoil sections.

The result of the thesis shows potential for the three investigated airfoil designs, though it has also been concluded that a closed single airfoil is a good design to begin with. In the focus span of 0 deg to 5 deg some open configurations were tested. When generating a lateral force the closed airfoil was the best one.

Keywords: Airfoil, Pylon, Aerodynamics, CFD, Optimization.

Acknowledgements

We would like to thank our supervisor Magnus Urquhart at Chalmers, without whom this thesis would never have gotten as far as it did. Thank you Magnus for putting up with our endless questions! We would like to thank Ugo Riccio and Vincenzo Sepe at Lamborghini for guiding us in the right direction and providing valuable input throughout the thesis.
We would also like to thank our examiner Lennart Löfdahl for supporting us with our thesis and for our many interesting conversations, both in the topic of the thesis as well as in motorsports.

Oskar Hellsten & Oskar Pettersson, Gothenburg, June 2020

Contents

List of Figures

1 Introduction

Today, nearly all aspects of a sports car are engineered down to its finest detail to have the best available performance which allows the manufacturers to bring down the lap records to groundbreaking times.
An area that is not at the final engineering stage is the pylons connecting the rear wing to the vehicle. Therefore a study on the possible benefits of a new design of the pylons was made in collaboration between Lamborghini S.p.A. and Chalmers University of Technology.

1.1 Background

Lamborghini S.p.A has the lap record for road legal production cars on the Nürburgring Nordschleife racing track, which proves that they are at the leading edge of the sports cars available on the market.
To be able to push a sports car to the absolute limit each element needs to be fine-tuned. One of the areas with potential of improvement is the pylons connecting the wing to the vehicle body. The investigation of the possible improvement of the pylon will hopefully lead to the creation of a new Lamborghini that one day will set a new lap record around the Nordschleife circuit.
Existing pylons of today are there for structural reasons and are not investigated from an aerodynamic perspective. Lamborghini has noticed that the pylon has not received enough attention and has decided that an investigation in the matter is needed.
The theory of wing sections is explained in (Abbott & Doenhoff., 1959) and includes a large number of tested wing profiles with corresponding plots on their performance at different angles of attack. There are studies that cover boundary layers, critical speeds that is of interest and their effect on the performance of the wing profile. It also includes graphs that show the performance of the commonly known family of airfoils designed by the National Advisory Committee for Astronauts (NACA) and the theory about them.
Studies on various setups on how to design a rear wing for a race car is done in (McBeath, 2015). Studies and explanations showing the effect of having a multi-section wing profile, end plates and other ways of improving the aerodynamics of a vehicle. General knowledge of the aerodynamics of a competition car is explained further.
In the aviation industry, many different designs have been tested to improve the lift of an airfoil and this knowledge has been transferred to the race car industry. In (Katz, 2006) the effects of a slat, flap, vortex generators and similar add-ons are explained.
Shahrooz Eftekhari (Timmer, 2010) investigated the correlation between wind tunnel measurements, reference data and Computational Fluid Dynamics (CFD) predictions with a NACA0012 airfoil as base. The tests are performed with different

angles of attack and with low Reynolds's number. The conclusion that is being drawn when comparing the three sources of data is that with increasing angle of attack the prediction accuracy of the simulations is reduced.

1.2 Purpose

The purpose of this thesis is to make an aerodynamic investigation of possible designs of the pylon connecting the wing to the car body of a Lamborghini. The investigation should aim to reduce the drag of the pylon, over a spectrum of wind attack angles, while at the same time exploring the possibility of creating a lateral force that can be utilized while cornering to improve the vehicle dynamics.

1.3 Question formulation

In accordance with the purpose of the project, the following questions are to be investigated:

- Could cornering aerodynamics efficiency and wing efficiency be improved with a new design of the pylons?
- For pylon use, is it possible to design a 2D-airfoil with good performance while improving efficiency at increasing attack angle using passive control?
- Can passive control be used on the airfoil, and where should it be located in the streamwise direction?
- Is it possible to use the passive control for reducing the thickness of the 3D-separated area at the contact between pylon and rear wing?
- Is there a way, using CFD simulations and optimization tools, to create a new pylon shape more effective than the conventionally used NACA airfoils?

1.4 Limitations

This project is limited to 20 weeks and due to the restricted amount of available time, this project only looks into a passive aerodynamic system and not an active one. The project will be conducted using 2D simulations since that is faster and will allow more options to be investigated.

2 Methods

Throughout this report, normalized values will be used.

2.1 Simulation prerequisites

Before any simulations were made, the mesh and domain that were to be used were investigated to see if they were reliable.

2.1.1 Mesh study

To find a balance between the number of cells and the output results of the simulation a mesh study was conducted. The goal was to find out when the result converges and does not change noteworthy with a finer mesh. The closed optimized airfoil set to an angle of attack of 5 *deg* was used in the analysis. The results of the study can be seen in figures 2.2 and 2.1.

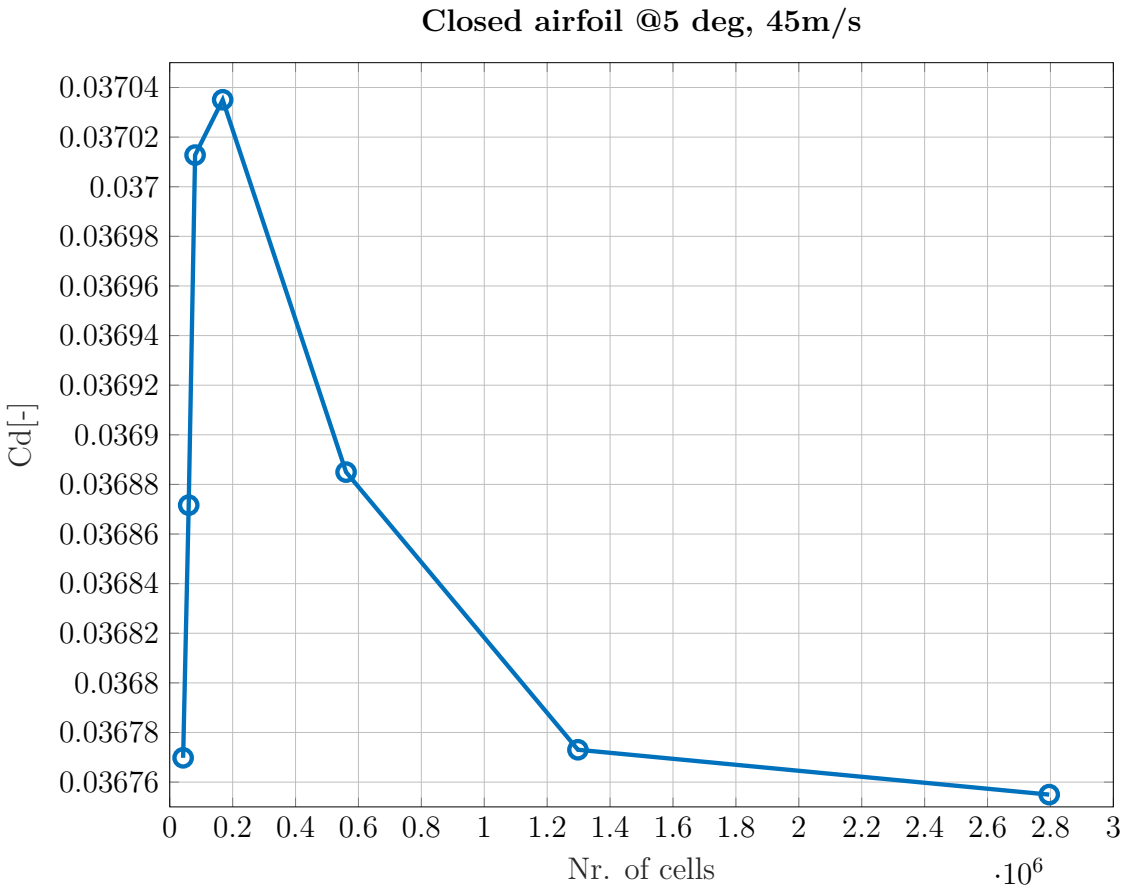

Figure 2.1: Resulting Cd value with a varying cell count

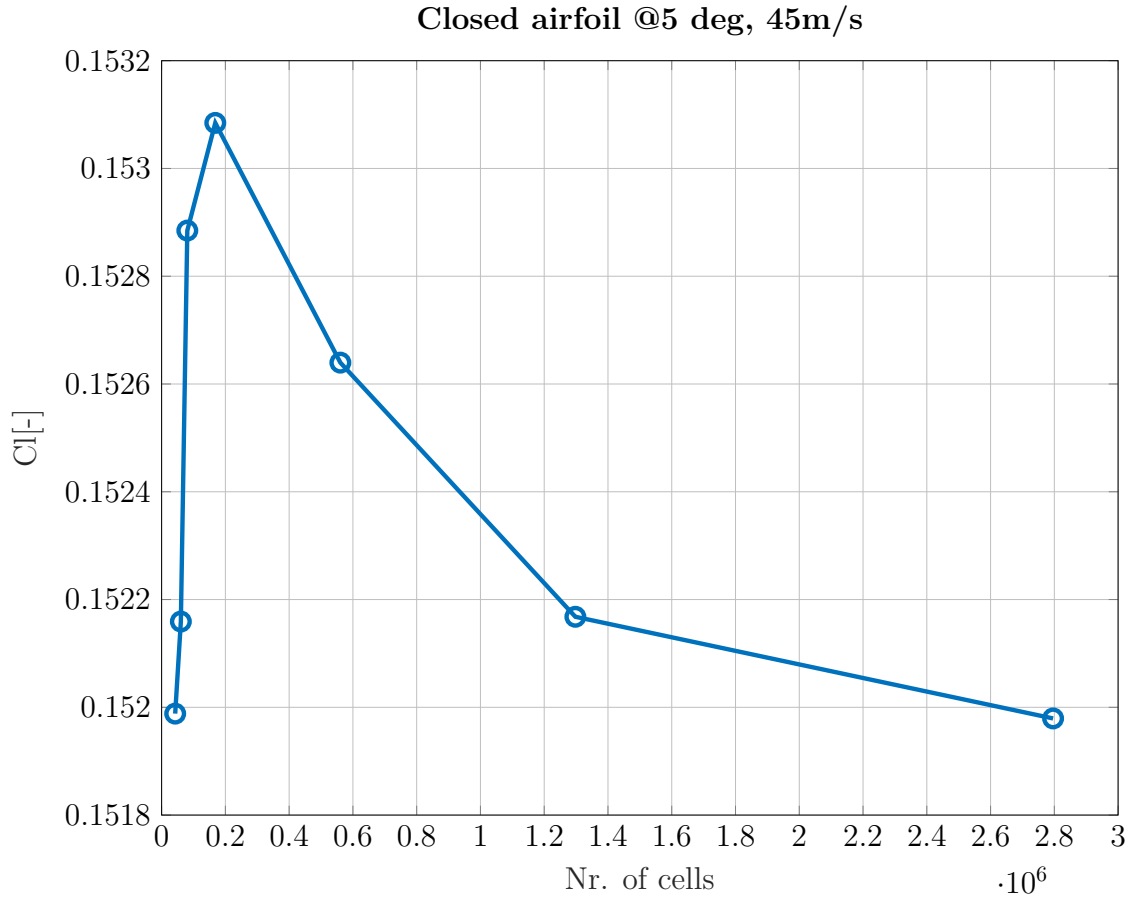

Figure 2.2: Resulting Cl value with a varying cell count

A polyhedral mesh is used due to that it is commonly used and is computationally cheap when simulating. To achieve the desired results a mesh with 60,000 cells was used and the mesh domain with refinement area can be seen in figure 2.3b and the mesh around the airfoil can be seen in figure 2.3a. By looking at the results from the mesh study it was chosen to go with the size that gave 60,000 cells, since values do not change very much and an increased amount of cells would lead to longer computation times. The difference of the Cd value between 60,000 and 2.8 million cells is approximately 0.0001 which is equivalent of 0.3 %, the same difference for Cl is approximately 0.001 which is equivalent of 0.007 %.

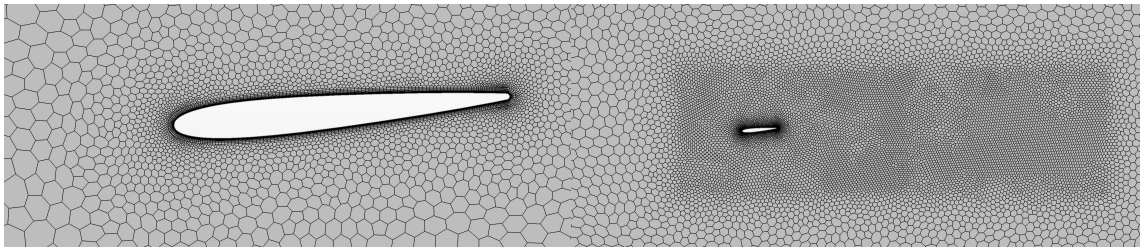

(a) Mesh around closed airfoil **(b)** Mesh in domain

Figure 2.3: Image showing the mesh around airfoil and in domain

2.1.2 Domain study

Much like the mesh study, the domain size was evaluated in order to make sure that it was large enough not to affect the results.

2.2 Lap time simulation

To determine the range of the angle of attack of a vehicle going around the Nürburgring Nordschleife race track experiences a lap time simulation was used. By using this simulation as a base it was possible to modify it so that the attack angle could be calculated for an entire lap.

2.2.1 Software

The angle of attack of the wind acting on the pylon can be calculated as shown in equation 2.1

$$AOA = tan\frac{\omega_z * x + V_y}{V_x} \tag{2.1}$$

Here the ω_z is the yaw rate, x is the distance from the center of gravity (CoG) to the center pylon seen in figure 2.4, V_y is the lateral velocity and V_x is the longitudinal velocity.

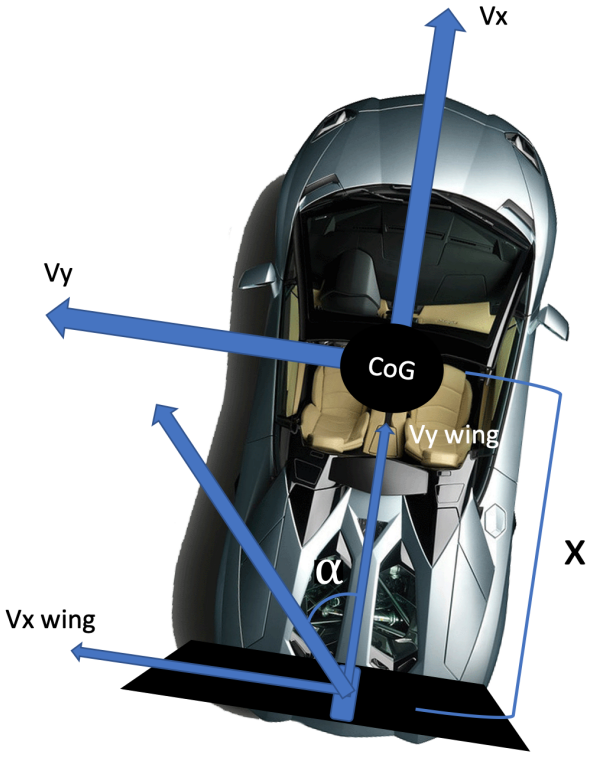

Figure 2.4: Schematic figure of forces to calculate angle of attack

A mass point is used in the lap simulator to simulate the vehicle when it is going around the track. At all times the lap time simulator uses the maximum performance available of the tire and vehicle combination. This is done by simulating forwards and backwards in time to determine the highest possible vehicle acceleration. The point mass follows a constant line from a desired track and does not consider the width of the track.

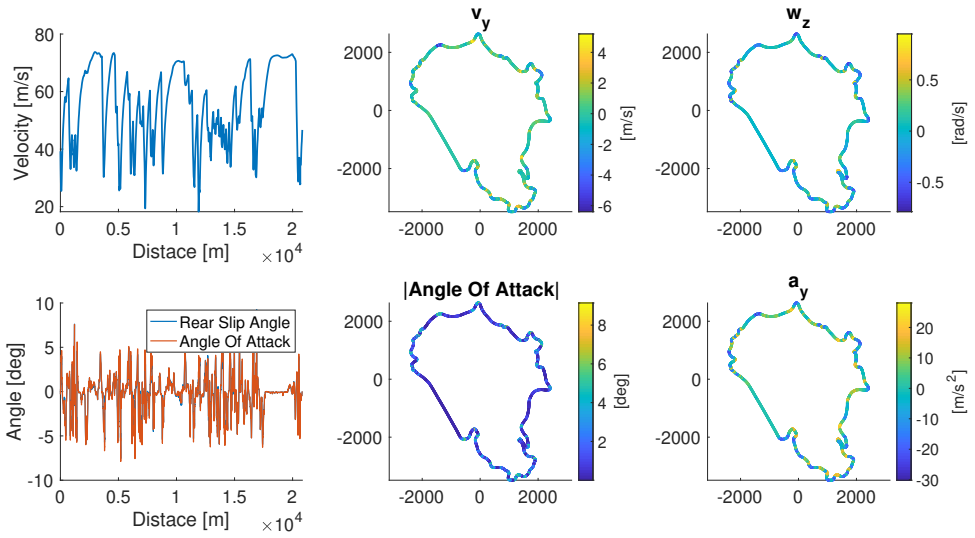

Figure 2.5: Generated plots from data calculated in lap time simulator

Interesting parameters from the lap time simulator can be seen in figure 2.5, such as the lateral acceleration seen to the down most right, the largest values can be seen in the sharp corners where the vehicle is limited by the available grip in the tires. Other parameters as the lateral velocity, yaw rate, angle of attack, velocity and rear slip angle can also be seen in figure 2.5.

Each angle of attack of the wind on the rear pylon is calculated for each instant during a lap, the data generated from the lap time simulator is then plotted together in a histogram. From the histogram in figure 2.6 it is possible to see that the most common angles of attack are between 0 *deg* and 5 *deg*. When optimizing the pylon design, angles of attack of 0 and 5 degrees were used based on this result.

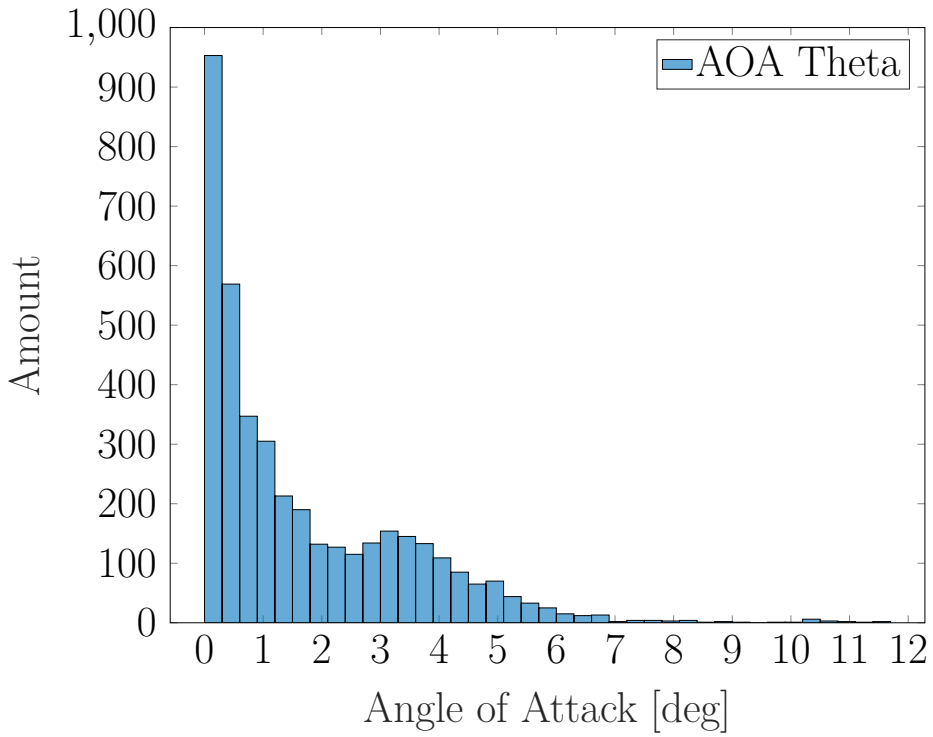

Figure 2.6: Histogram of angle of attack during a lap around Nordschleife

2.3 Airfoil development

2.3.1 Initial airfoil decisions

There has been substantial research into airfoil shape and design throughout the last century and therefore there is a large amount of data available. It is therefore suitable at the beginning of the project to use the shapes of already existing airfoils. Through an airfoil tool (AirfoilTools, 2020) available on the web existing airfoils could easily be compared on their shape and performance. The basic parameters of an airfoil can be visualized in figure 2.7.

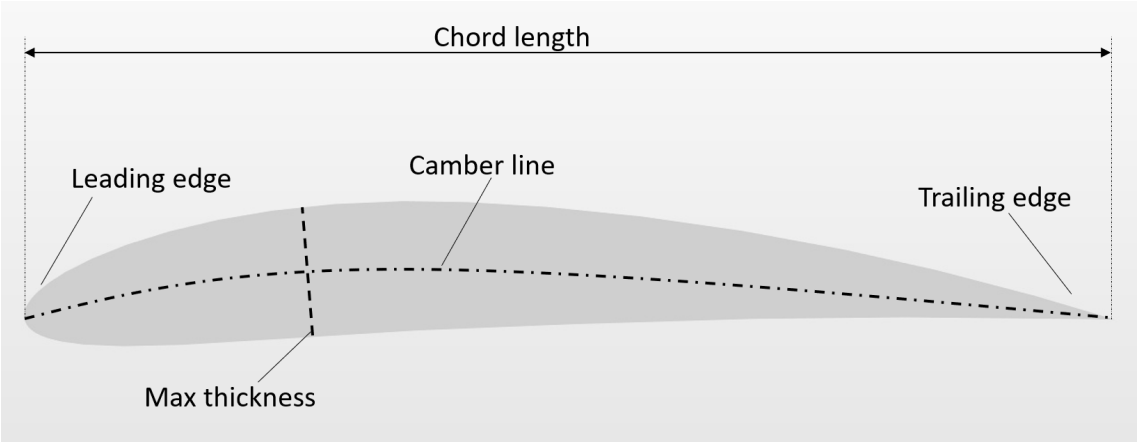

Figure 2.7: Basic parameters of an airfoil

The airfoil that is the pylon should not be sensitive to if the angle of attack of the oncoming flow is positive or negative in the car's coordinate system. Therefore it was decided in an early stage that a symmetric airfoil was the most appropriate to use.

It was concluded that a span of the angle of attack from 0 *deg* to 5 *deg* was the most relevant spectrum to focus the performance of the airfoil on, but that is not including the factor of the wind. If there is a side wind acting on the vehicle the angle of attack of the wind might be larger than 5 *deg*, therefore the investigated range will be increased in order to make sure that the performance of the airfoil does not fail if the angle of attack should exceed 5 *deg*. Another aspect that further strengthens the idea of the increased range is the side slip angle of the vehicle. If the vehicle gets lateral side slip it can cause the angle of attack acting on the pylon to be increased. With this in mind angles of attack up to 15 *deg* will be investigated, though the focus will still lie in the 0 *deg* to 5 *deg* range.

2.4 Coordinate system

When doing tests in a wind tunnel the most common case is to rotate the object being tested in the tunnel to get the desired angle of attack of the wind, not changing the attack angle of the wind approaching the object. But when looking at a road-going vehicle it is often more beneficial to investigate the acting forces in the vehicles local coordinate system. In figure 2.8 it is possible to see the two cases of global and local coordinate systems.

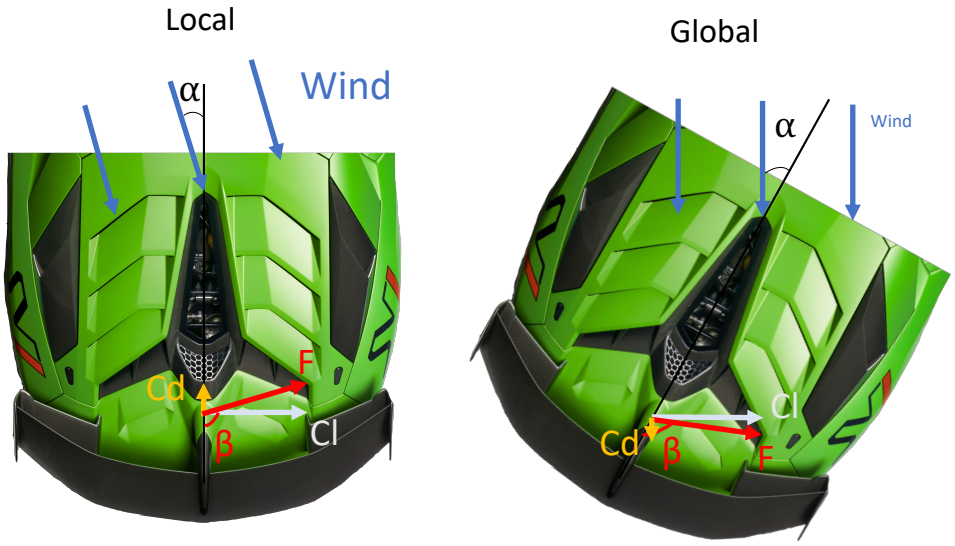

Figure 2.8: Local and global system configuration

With that in mind and with the knowledge that the focus of this thesis is the forces acting on the vehicle, the planned simulations and optimizations were to be done in the local system of the car and by such also the pylons. The difference in Cd when using local and global systems is shown in figure 2.9, where it is possible to see that the Cd value goes from positive to negative.

Using the local coordinate system of the car will lead to that a left-hand turn will create a negative lift when looking at the pylon, in the same way a right-hand turn will result in a positive lift force on the pylon. Since the airfoil will be symmetric the result from one direction will be the same in the other one, for simplicity only one direction is therefore investigated.

While cornering the resulting force from the pylon will point inwards to the corner, and in that case, put more load on the inner wheel. This will lead to that the outer tire gets less load and will get less saturated and the inner wheels can take more of the load instead, so a higher total amount of grip while cornering will be achieved.

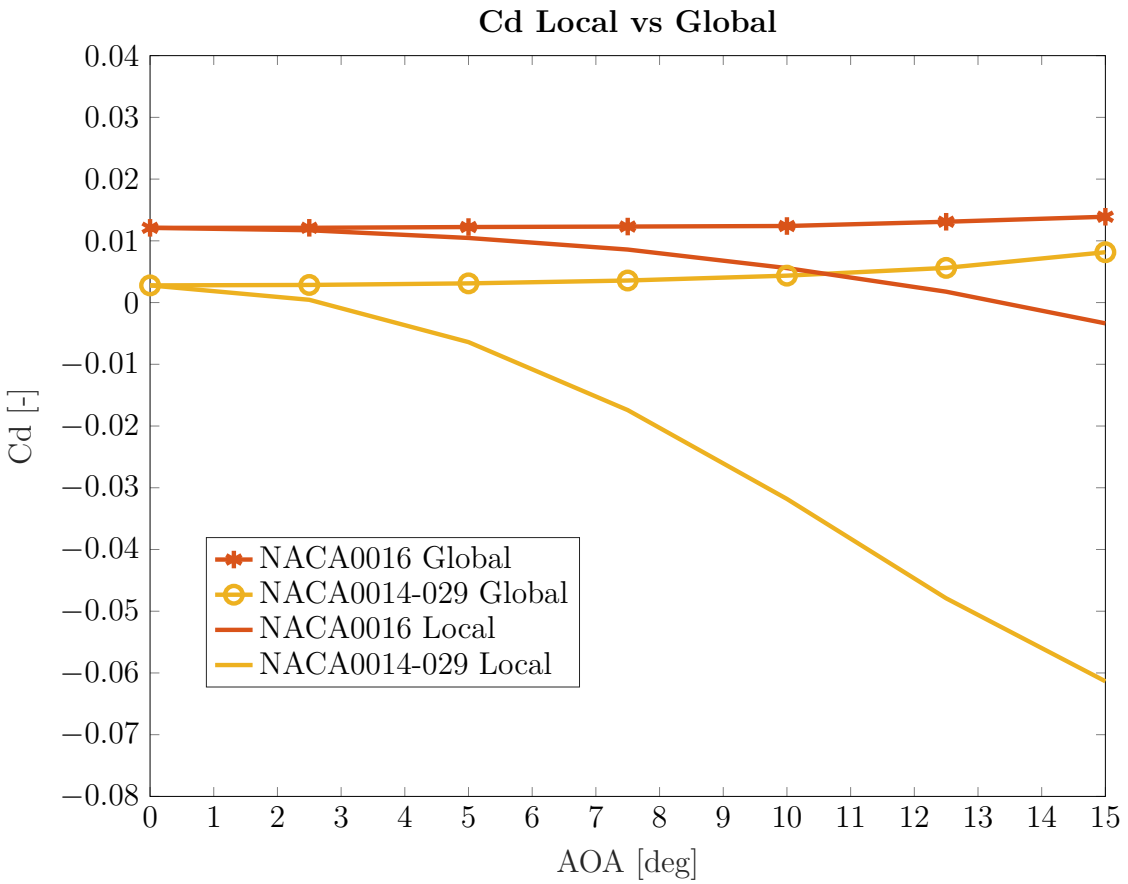

Figure 2.9: Plot of local and global Cd

The phenomena with negative Cd can be recognized from sailing boats that are sailing towards the wind. When increasing the angle of attack of the wind there will be a certain angle where the drag reduces to negative, and by such propelling the boat forwards. The cost of being propelled at this angle is a relatively large lateral force acting on the vehicle, whether that be a sailing boat or a car.

When looking at the Cl in the local and the global system the difference is not as visible, due to the lift force is much larger in total, as can be seen in figure 2.10.

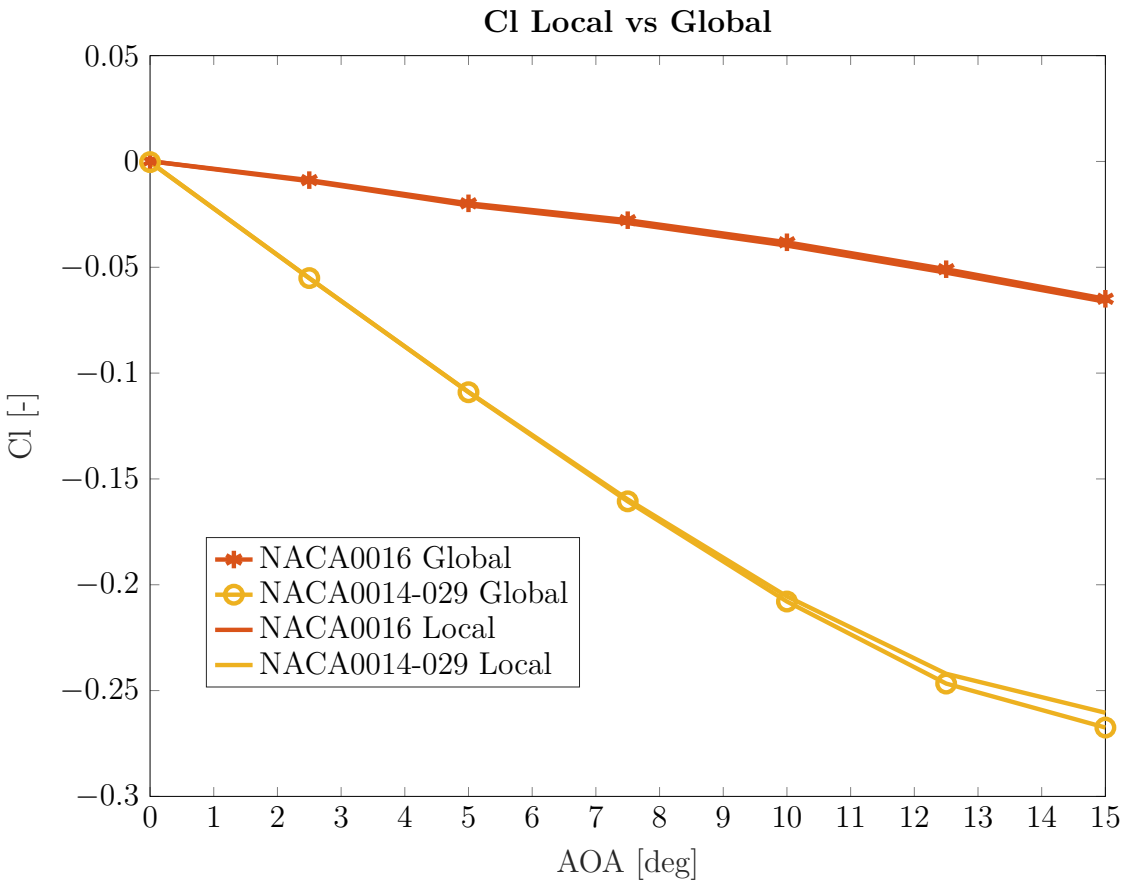

Figure 2.10: Plot of local and global Cl

2.4.1 The quest for the optimal airfoil

Airfoil selection and optimization are typically performed relate to the motion of the airfoil, for example in the use of aircraft, the lift is evaluated perpendicular to the ground. In this work, the desired effect of the pylon airfoil is to improve lateral and longitudinal performance of the vehicle. Because of the unusual operating conditions as well as the requirement of the airfoil being symmetric, the shape of the airfoil was optimized, instead of selected from the vast numbers of airfoils available in the literature.

The maximum thickness, chordwise location of the thickest part of the airfoil, leading edge radius, angle of trailing edge boat-tail and airfoil length was optimized using the software provided by Cesar Galan (Galan, 2020). In figure 2.11 it is possible to see some of the airfoils that can be created with the software. The minimum radius of any corner on an airfoil was set to 2.5 mm and the minimum thickness of the thickest part of the airfoil was set to 30 mm due to structural matters.

Three different targets were set up optimize towards, low drag at 0 deg of attack angle, high lift at 5 deg of attack angle and low drag at 0 deg and 5 deg of attack angle. To optimize for low drag at both 0 deg and 5 deg of attack angle a weighted value was created, where 50% of the drag of each angle was combined. The goal of

the optimization was then to minimize the weighted value.

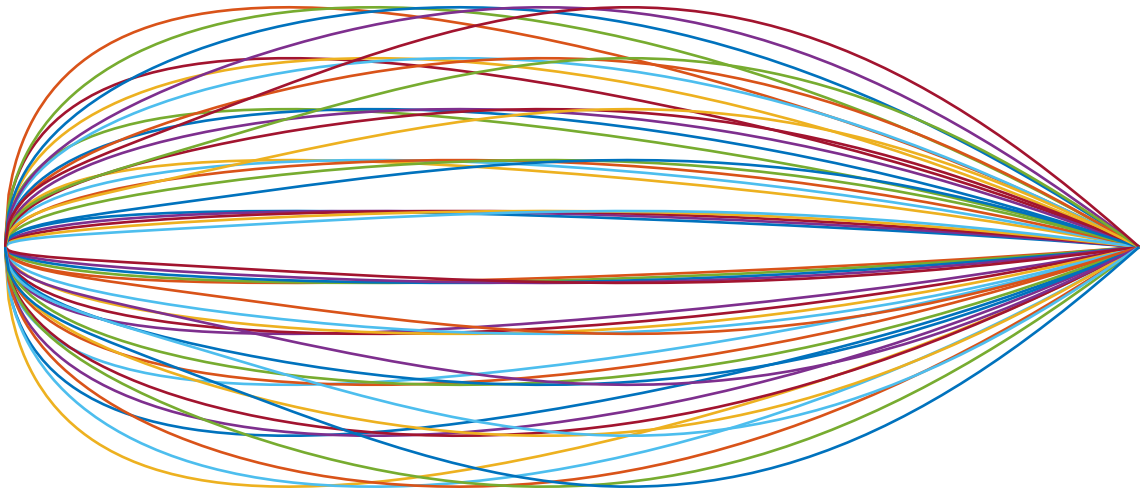

Figure 2.11: Airfoil creator in Matlab

A simple flow chart of the optimization loop can be found in figure 2.12. The entire optimization process is running through the Julia programming environment in this project (Jeff Bezanson, 2017). The optimization loop is based on a surrogate model in order to reduce the number of CFD simulations needed, as the model creates a base on which the following iterations are built from. The algorithm tries to investigate areas where the model uncertainty is large as well as looking into already well performing areas (Magnus Urquhart, 2020).

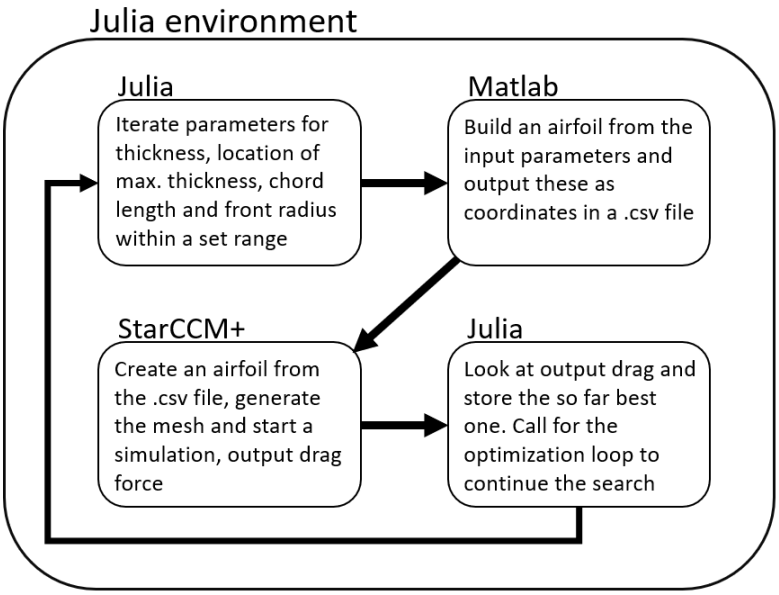

Figure 2.12: Flow chart of the utilized optimization loop

2.4.2 Optimization for the best slots

Using the airfoil found in the first step of the process, different designs of the slots were tested to investigate the initial behavior of the flow around and through the airfoil. Which lead to the definition of the parameters that were used in the optimization of the slotted airfoil, though the different parameters are confidential. The goal was to guide air from the high pressure side of the airfoil to the low pressure side and accelerate the flow on the low pressure side. The idea is to overcome the positive pressure gradient so the flow does not detach. By using the optimization tool it was possible to investigate a large number of configurations and find the best one out of those.

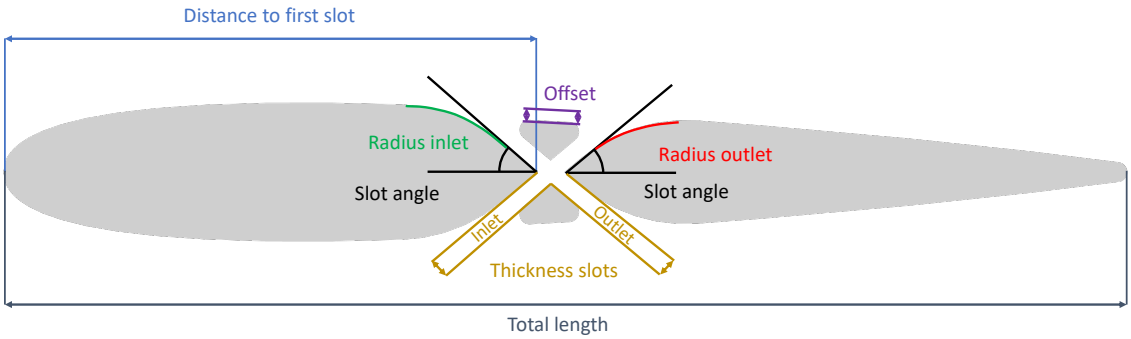

Figure 2.13: Variable parameters that were used in the optimization loop

Each of these parameters had a range in which the value of a said parameter is

allowed to be. This range was set with the intent to keep the slots in a feasible area of the airfoil and also to reduce the number of iterations and time it takes to run a full optimization.

2.4.3 Sensitivity analysis of slotted design

In order to find out which of the seven parameters shown in figure 2.13 that are the most influential on the performance of the airfoil, a sensitivity analysis was made. Each of the parameters was changed individually within the predetermined range, while the other ones were kept in the middle of their respective range. Each parameter was tested for five values; the two extremes of the range, the middle, and one step between the extreme and the middle in both while keeping the other parameters in the middle of the range. In this way, it was possible to find which parameter had the largest individual effect and at which part of the range it performed the best.

2.4.4 Double Airfoil

With inspiration from the formula race cars of today that are equipped with multi slotted wings, a double airfoil design was created. On formula cars, the idea of a multi slotted wing is to have a large camber of the total wing, but for the intended use as a pylon the airfoil in this thesis will be symmetrical. Similarly to the closed airfoil, the maximum thickness, chordwise location of the thickest part of the airfoil, leading edge radius, angle of trailing edge boat-tail and airfoil length parameters of both airfoils was optimized as well as the gap between the two airfoils In figure 2.14 it is possible to see what a double airfoil can look like.

Figure 2.14: An example of the shape of a double airfoil

Just like with the closed airfoil and the slotted design the double airfoil was optimized in order to find the best set up for the two wing sections. When setting up the optimization script the front and rear airfoil was given different range on the available parameters. This was made due to that there are some minimum measures and reference values that needs to be kept in mind. Each airfoil is separated from the other and can take on its own shape, the distance between the airfoils can vary as well. As seen in figure 2.14 the front and rear airfoil have totally different shapes, but together they are optimized for minimum drag at 0 deg and 5 deg.

3 Results

3.1 Optimization of airfoil shapes

In the optimization three different targets were set up to optimize towards, lowest drag at 0 *deg*, lowest drag at 0 *deg* and 5 *deg* and highest lift at 5 *deg* of attack angle. In table 3.1 it is possible to see the range of the parameters that were used when optimizing each airfoil, the parameters have been scaled to a 1 m long airfoil.

In figure 3.1 it is possible to see the airfoils generated from the optimization together with NACA airfoils that have the same length to width ratio as the drag optimized airfoils. The shapes of the optimized airfoils compared to the NACA airfoils are very similar, with small geometrical differences between them.

Parameters	Airfoil	Unit
Maximum thickness	0.1 - 0.23	[-]
Chordwise location of maximum thickness	0.84 - 1.84	[-]
Relative quantity of leading edge radius	1 - 2	[-]
Relative quantity of trailing edge boat-tail angle	6.34 - 7	[-]
Length of airfoil	0.57 - 1	[-]

Table 3.1: Range of scaled parameters for the closed airfoil

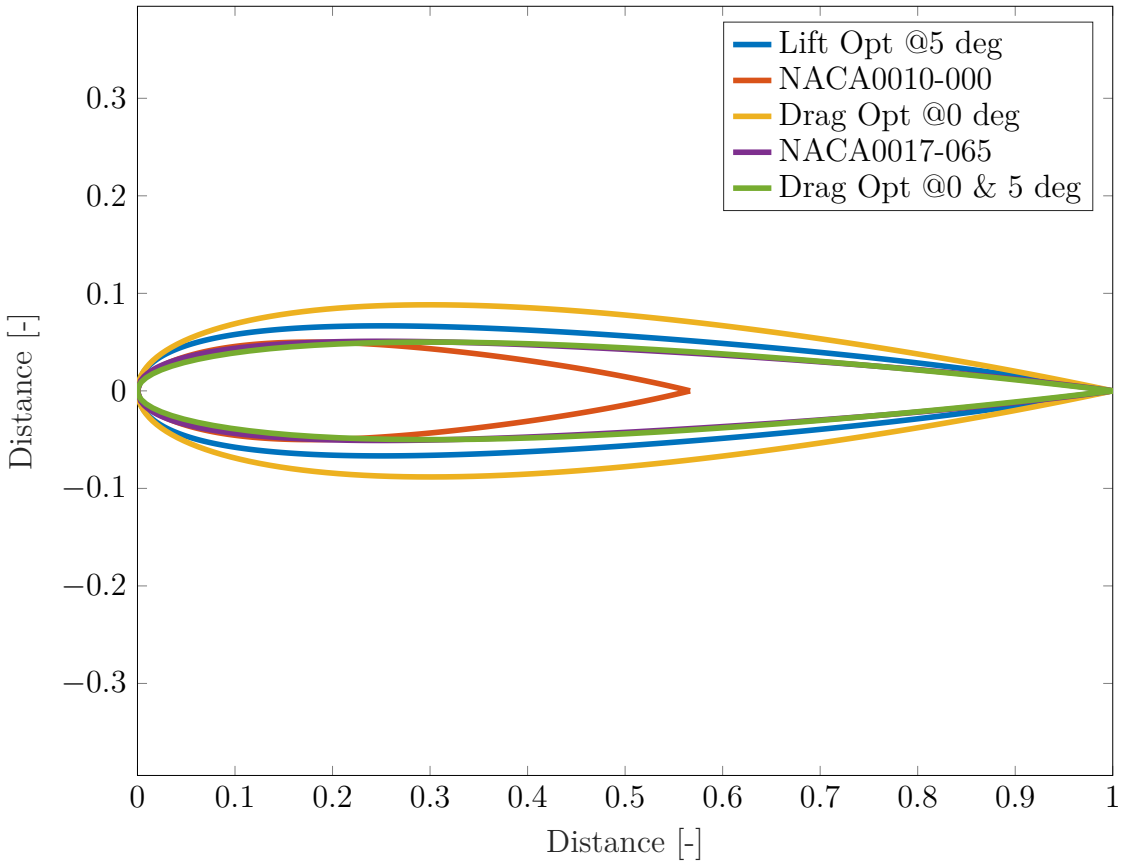

Figure 3.1: Shapes of optimized airfoils and NACA airfoils

The optimization history of the closed single airfoil can be seen in figure 3.2, as can be seen in the graph the solution converges quite fast as the value does not change throughout the iterations, the function value for this optimization was drag.

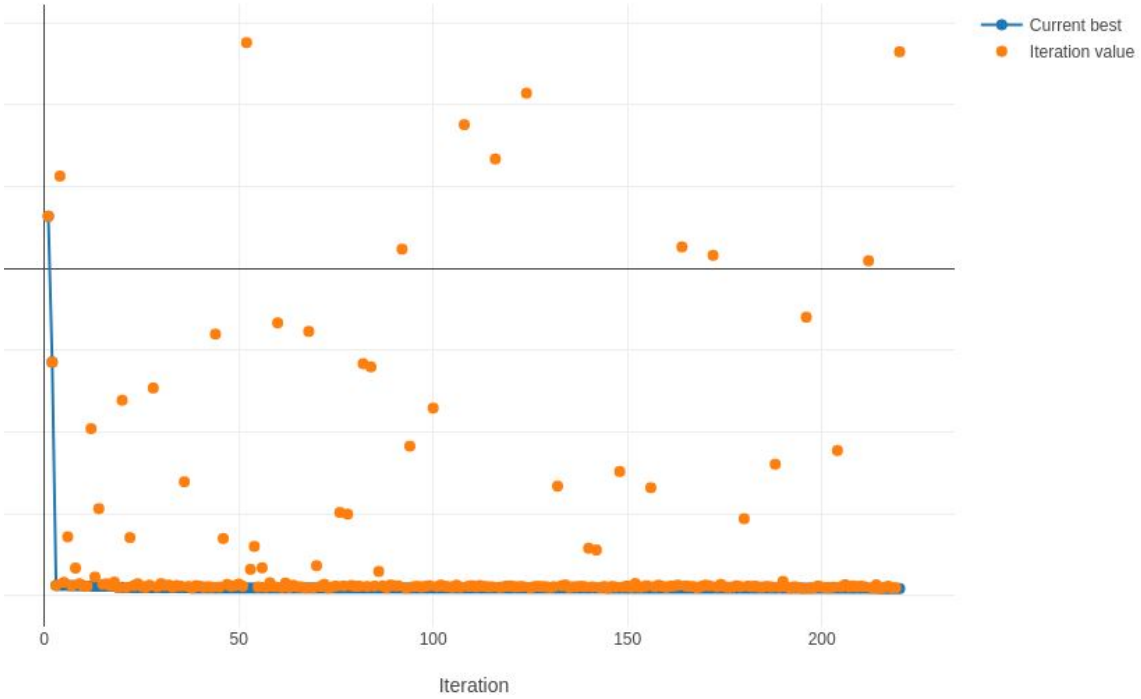

Figure 3.2: Optimization history of the closed airfoil

When looking at the Cd for each airfoil all of them perform similar up to 3 *deg* of attack angle except the NACA0010-000 airfoil that has a bit lower drag. At larger angles the *drag optimized at 0 deg* and the NACA0017-065 airfoil does not have as steep of a curve as the one optimized for lift at 5 *deg* and *drag optimized at 0 deg and 5 deg*. The NACA0010-000 performs well from 0 *deg* until 5 *deg*, and beyond there it looses performance compared to the *drag optimized at 0 deg and 5 deg* and the *lift optimized at 5 deg*. From 7.5 *deg* and further the flow around the NACA0010-000 airfoil separates and it therefore gets reduced performance.

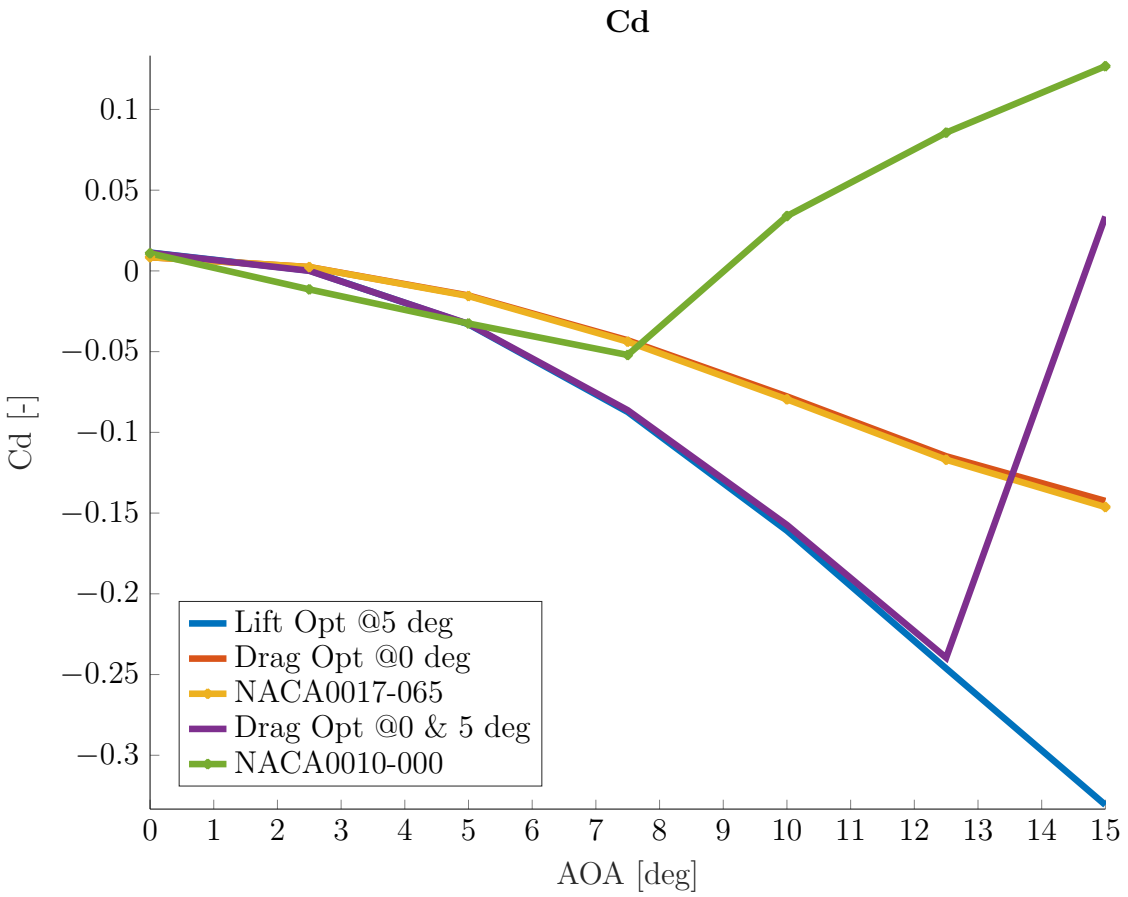

Figure 3.3: Cd for each airfoil in figure 3.1

The investigation of the Cl of the different airfoils lead to some results. Looking at the drag optimized airfoil at 0 *deg* and the NACA0017-065 they have less lift compared to the other three airfoils when increasing the angle of attack. This is due to the shorter chord length compared to the other airfoils that can be seen in figure 3.1. Comparing the *lift optimized airfoil at 0 deg*, NACA0010-000 and the *drag optimized at 0 deg and 5 deg* they perform similarly. But the lift optimized performs slightly better, which is not so strange since that is what it is optimized for. Both the *drag optimized at 0 deg and 5 deg* and NACA0010-000 gets reduced performance at 12.5 *deg* and respective 7.5 *deg* angle of attack due to that the flow around the airfoils detaches. The reason that both the lift optimized at 5 *deg* and the *drag optimized at 0 deg and 5 deg* perform similarly is because an increased lift force gives an increased negative drag. Thus the optimization tool will try to make an airfoil that has a large lift on both cases.

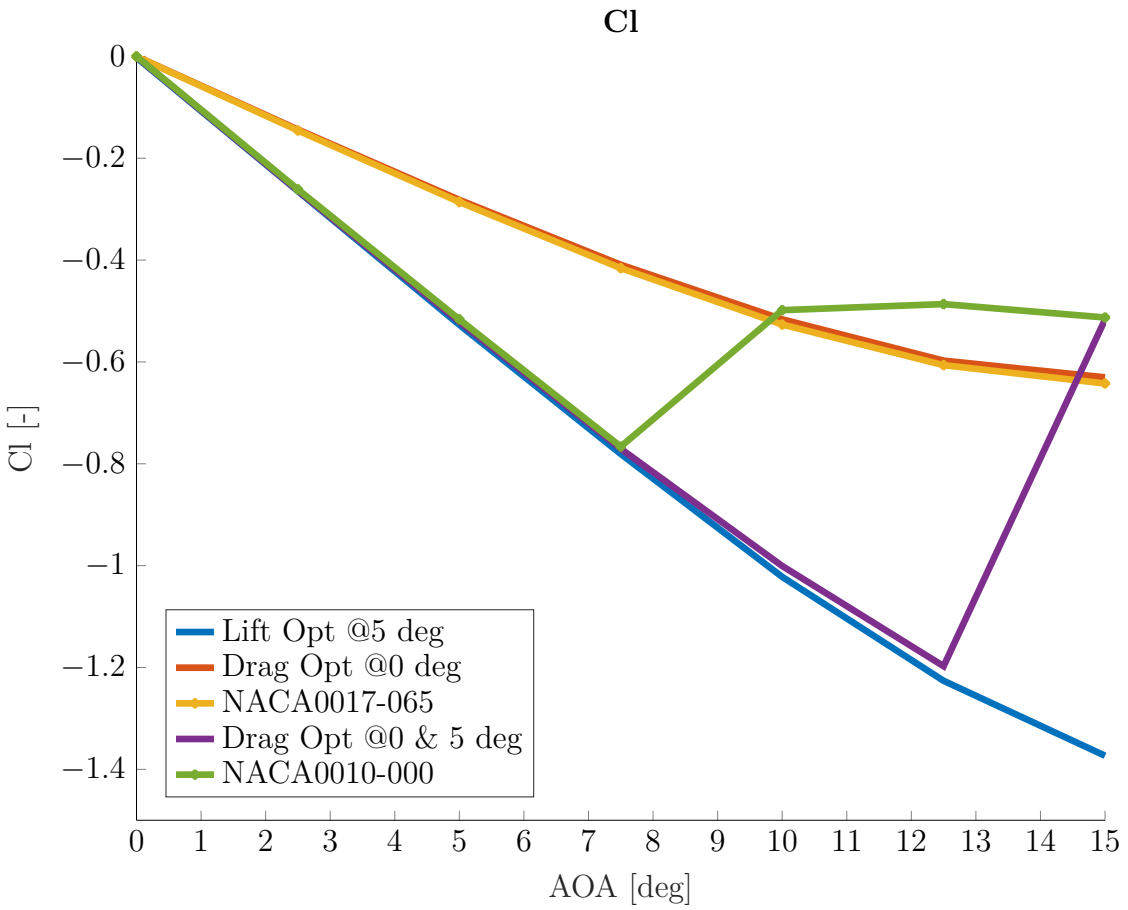

Figure 3.4: Cl for each airfoil in figure 3.1

From looking at figures 3.1 to 3.4 the decision was taken to use the drag optimized airfoil at both 0 *deg* and 5 *deg* for further development of the later added geometrical features.

3.1.1 Can you beat a NACA airfoil?

An in-depth comparison between a NACA profile with the same proportions as the created optimized airfoil was made. In figure 3.5 it is possible to see the shapes of the two compared airfoils. The front shape of the *drag optimized at 0 deg and 5 deg* is a bit rounder and the position of the thickest part of the airfoil is located more towards the leading edge compared to the NACA0010-000 airfoil. Looking from the center to the back of the airfoil the NACA0010-000 is a bit thicker, while the *drag optimized at 0 deg and 5 deg* has a different angle of the boat tail which makes it a bit narrower in the rear part.

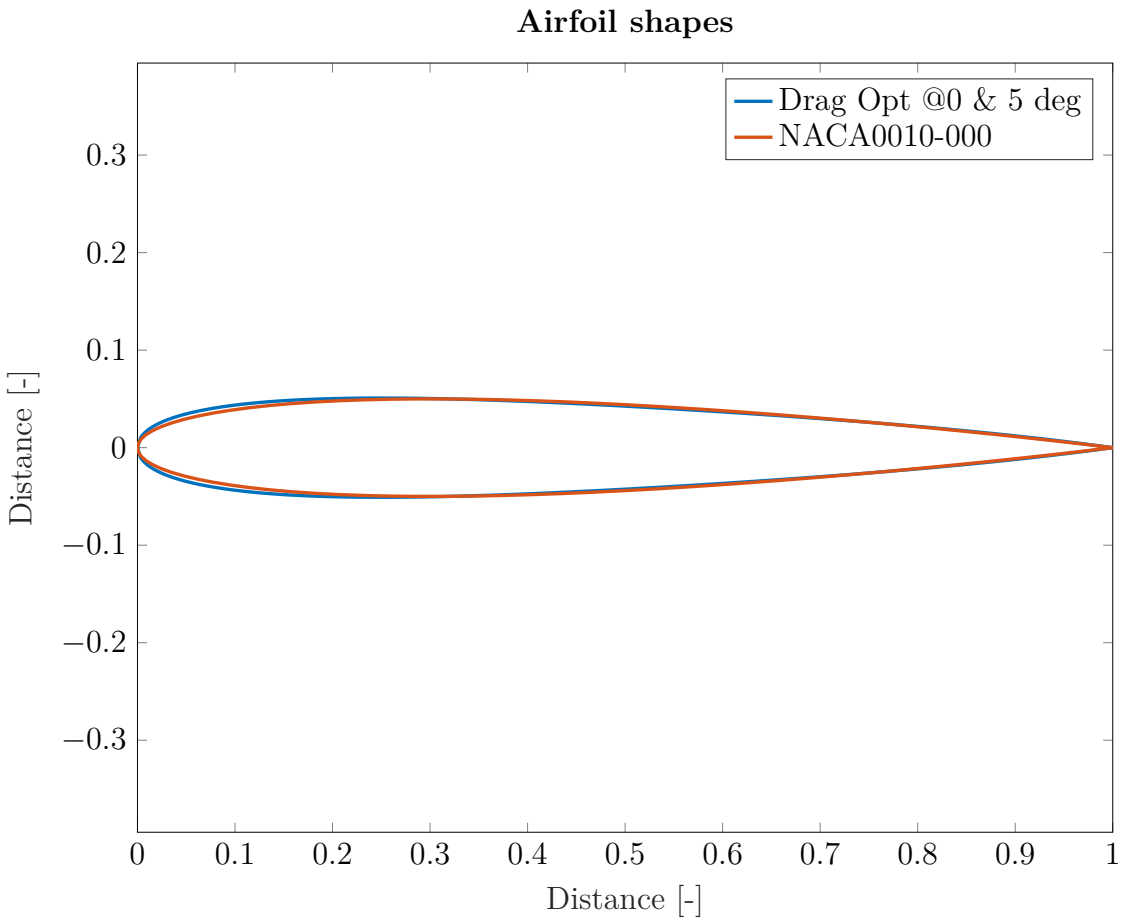

Figure 3.5: Shape comparison between NACA airfoil and generated airfoil

These small geometrical differences gives a difference in performance, as seen in figure 3.6a. The difference is small but the NACA airfoil performs a bit better than the *drag optimized at 0 deg and 5 deg* regarding drag in attack angles between 0 *deg* and 5 *deg*. At attack angles larger than 5 *deg* the *drag optimized at 0 deg and 5 deg* out performs the NACA0010-000 regarding having low drag.

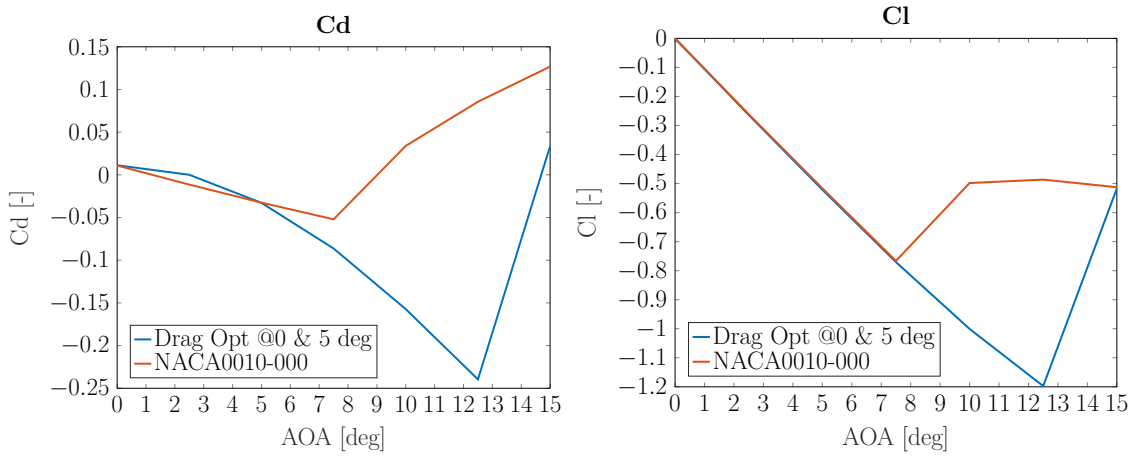

(a) Drag comparison **(b)** Lift comparison

Figure 3.6: Drag and lift comparison between NACA airfoil and drag optimised airfoil

Both airfoils perform similarly until 7.5 *deg* where the flow around the NACA0010-000 gets separated from the airfoil and loses performance against the *drag optimized at 0 deg and 5 deg*, on which the flow stays attached for longer. This is likely due to the more rounded leading edge on the drag optimized airfoil. In figure 3.7 it is possible to see how the flow has detached from the airfoil and a large low pressure area has been created.

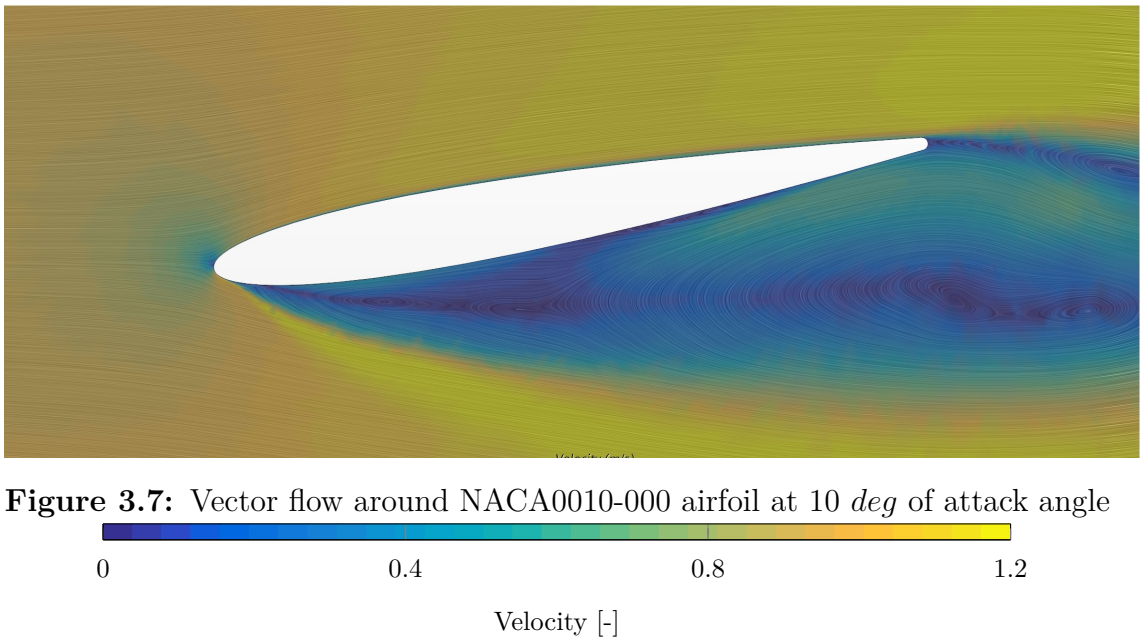

Figure 3.7: Vector flow around NACA0010-000 airfoil at 10 *deg* of attack angle

Parameters	Airfoil slots	Unit
Inlet radius	0.003 - 1	[-]
Offset	0.00013-0.0125	[-]
Outlet radius	0.003 - 0.75	[-]
Slot angle	20 - 60	[-]
Slot width of airfoil	0.013 - 0.1	[-]
Distance to first slot	0.038 - 0.25	[-]

Table 3.2: Range of scaled parameters for the slotted airfoil

3.2 Additional geometrical features

With the closed single airfoil that is optimized for 0 *deg* and 5 *deg* as a base, the investigation of alternative designs was conducted to see if the closed airfoil could be improved upon.

3.2.1 Slotted airfoil

This type of solution is an attempt to improve the airfoil by guiding air through it, especially when there is an attack angle of the wind acting on the pylon that is larger or smaller than 0 *deg*.

The result from the optimization of the airfoil where the goal was to reduce drag at 0 *deg* and 5 *deg* with added slots, can be seen in figure 3.8.

Figure 3.8: Slotted airfoil design generated from optimization

The optimization history of the slotted airfoil can be seen in figure 3.9, as can be seen in the graph the solution converges quite fast as the value does not change throughout the iterations, the function value for this optimization was drag. The goal was to reduce drag at both 0 *deg* and 5 *deg*.

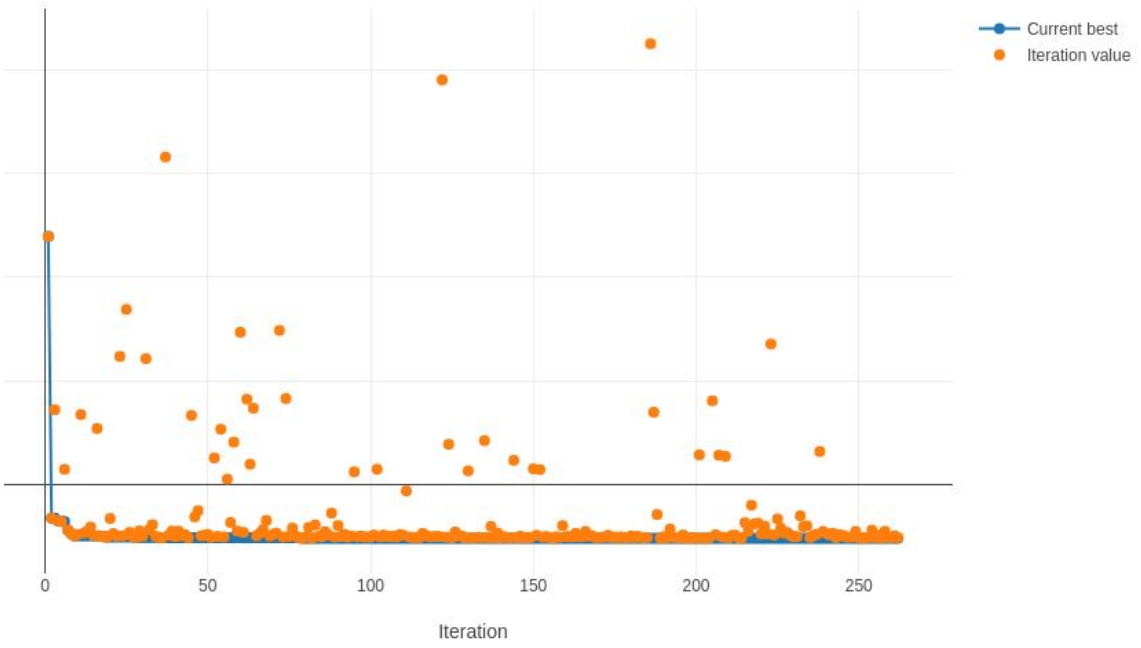

Figure 3.9: Optimization history of the slotted airfoil

It was concluded that the optimization of the drag at 0 *deg* and 5 *deg* have aimed to reduce the impact of the slots as much as it was allowed to. At 5 *deg* of attack angle, there is a small amount of flow that enters and passes through the slots. The drawback of that location is that it also minimizes the possible effect of the slots at larger angles of attack. Having the slots more to the leading edge would have a possible beneficial effect with helping to overcome the positive pressure coefficient on the low pressure side of the airfoil.

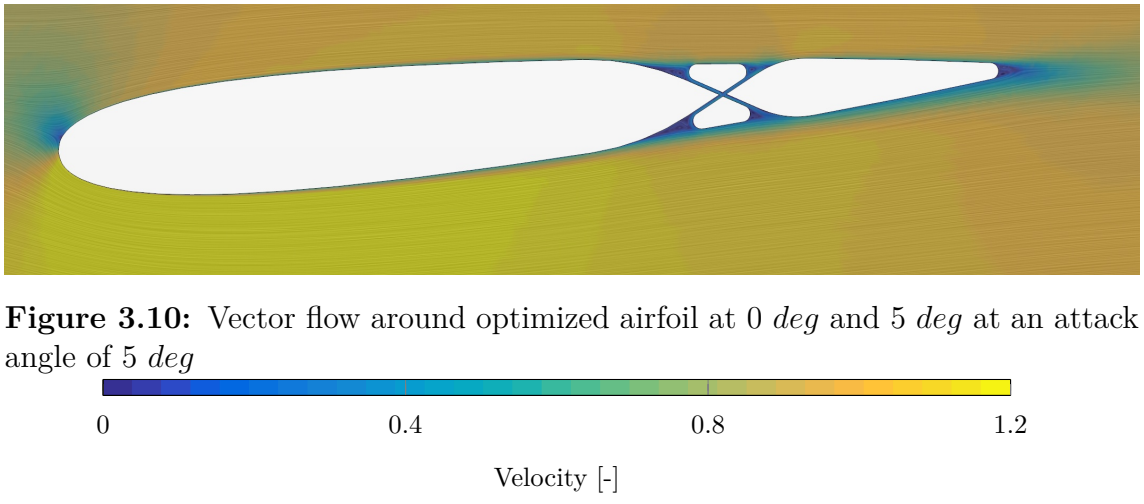

Figure 3.10: Vector flow around optimized airfoil at 0 *deg* and 5 *deg* at an attack angle of 5 *deg*

To see if the optimization had found the best values of the parameters in the region a local sensitivity analysis was done. Where two steps of 5% were taken in both negative and positive direction from the optimized value. The impact of each parameter can be seen in figure 3.11

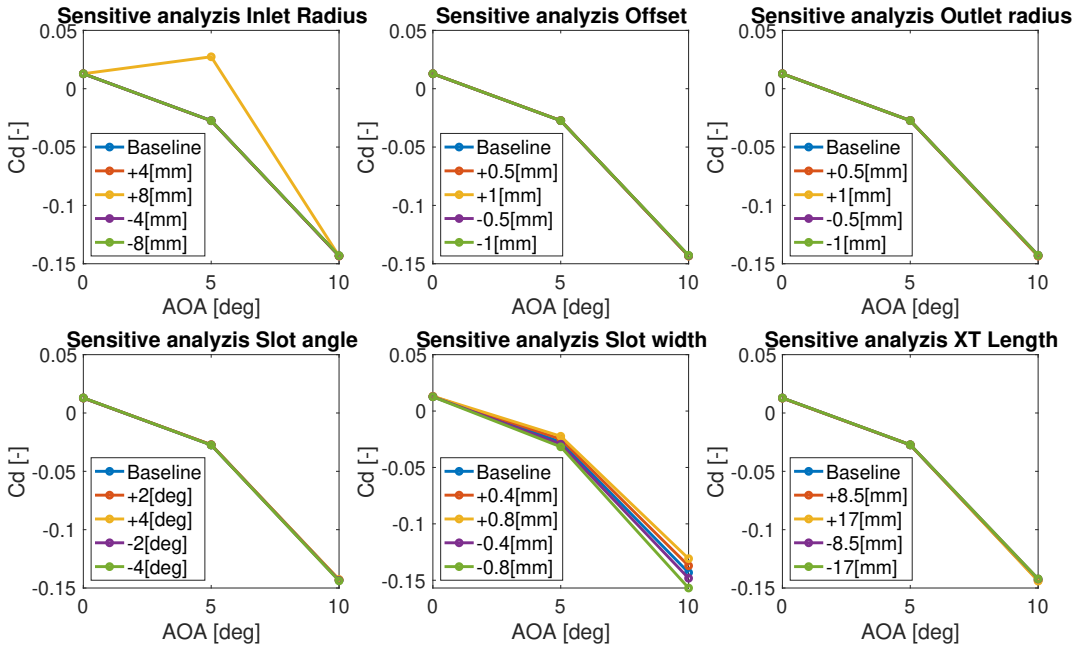

Figure 3.11: Plots from the local sensitivity analysis

The slotted airfoil that can be seen in figure 3.13 was generated from the sensitivity analysis that is shown in figure 3.12, the slots on this airfoil are located more to the center of the profile compared to the drag optimized airfoil at 0 *deg* and 5 *deg*.

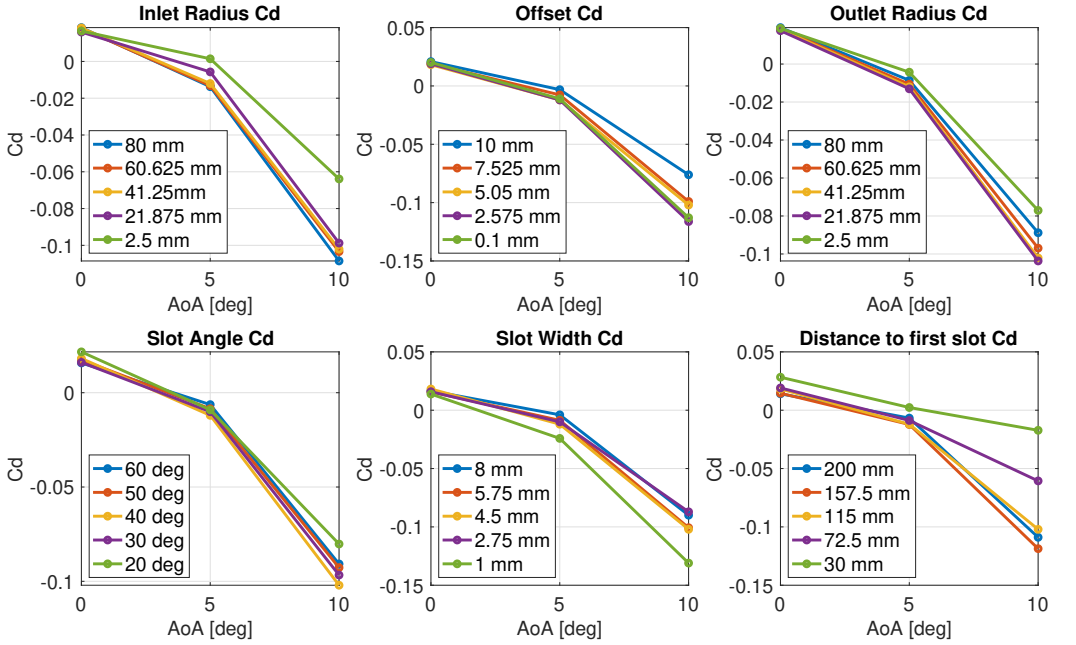

Figure 3.12: Plots from the global sensitivity analysis

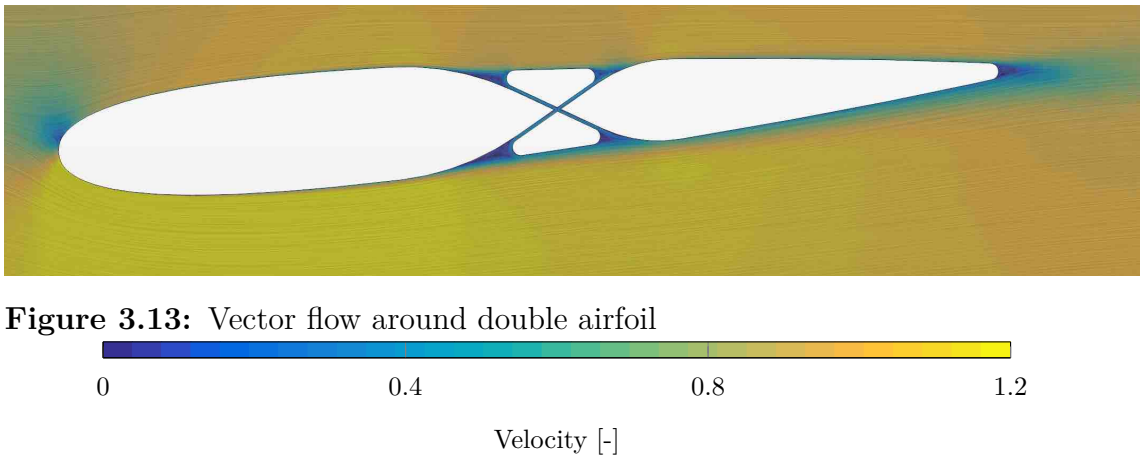

Figure 3.13: Vector flow around double airfoil

Another difference is that there is a larger inlet radius that will allow more flow to go through the slots, but since the slots are at their minimum thickness the amount of air passing through the slots will not be that large. The effect of accelerating the flow and avoiding the positive pressure coefficient on the low pressure side is not as beneficial as one might have thought.

3.2.2 Double airfoil

With inspiration from the formula race cars of today with multi slotted wings, a double airfoil design was created. In figure 3.14 the shape of the airfoil that was drag optimized at 0 *deg* and 5 *deg* is visualized.

Figure 3.14: Shape of double airfoil

The used range of each parameter for the two airfoils combining and creating the double airfoil can be seen in the table 3.3.

The optimization history of the double airfoil can be seen in figure 3.15, as can be seen in the graph the solution converges quite fast as the value does not change throughout the iterations, the function value for this optimization was drag.

Parameters	Airfoil 1	Airfoil 2	Unit
Maximum thickness	0.15 - 0.35	0.05 - 0.25	[-]
Chordwise location of maximum thickness	0.125 - 0.2	0.125 - 0.2	[-]
Relative quantity of leading edge radius	0.5 - 3	1.25 - 12.5	[-]
Relative quantity of trailing edge boat-tail angle	9.5 - 29.5	9.5 - 19.5	[-]
Length of airfoil	0.5 - 1.0	0.5 - 1.0	[-]

Table 3.3: Range of parameters for the double airfoil

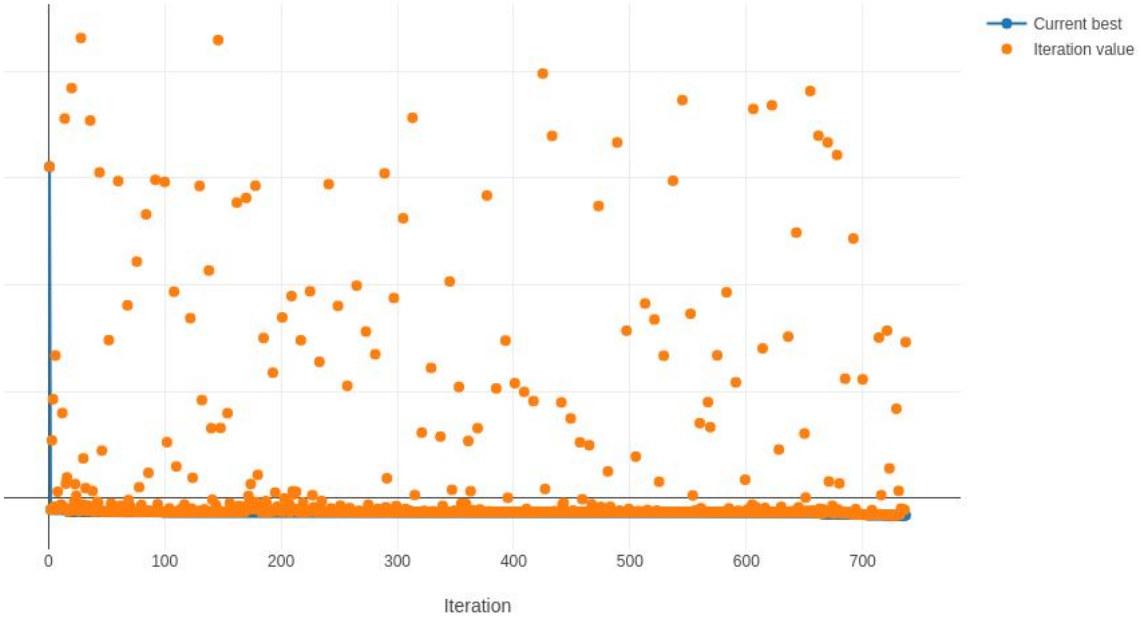

Figure 3.15: Optimization history of the double airfoil

Looking into the flow field around the double airfoil there is no flow going through the gap between the two airfoils at 0 *deg*. But at 2.5 *deg* of attack angle the air starts to flow through the slot, this can be seen in figure 3.16. Increasing the attack angle further leads to that flow with higher speed starts to flow through the gap, and in that way accelerates the flow under the second airfoil. This will lead to that the flow will stay attached to the airfoil due to that it is possible for it to overcome the positive pressure coefficient.

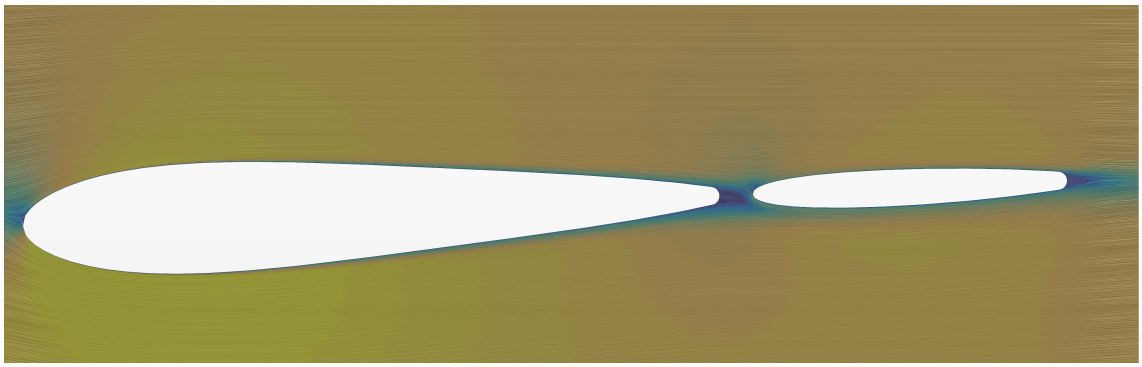

Figure 3.16: Vector flow around double airfoil

3.3 Comparison of created airfoils

After the simulations and the optimizations of the various airfoils the final four shapes of the airfoils can be seen in figure 3.17. Airfoil number one is a closed single airfoil which is drag optimized at 0 *deg* and 5 *deg* of attack angles, it is also used as the base shape for airfoil number three and four. Airfoil number two is a double airfoil with two different airfoils after each other that is optimized for low drag at 0 *deg* and 5 *deg* of attack angle. Airfoil number three is an airfoil with slots that are optimized for low drag at 0 *deg* and 5 *deg* of attack angle. The final airfoil, number four, has slots designed from the results of the global sensitivity analysis where the best value for each parameter was taken and put together.

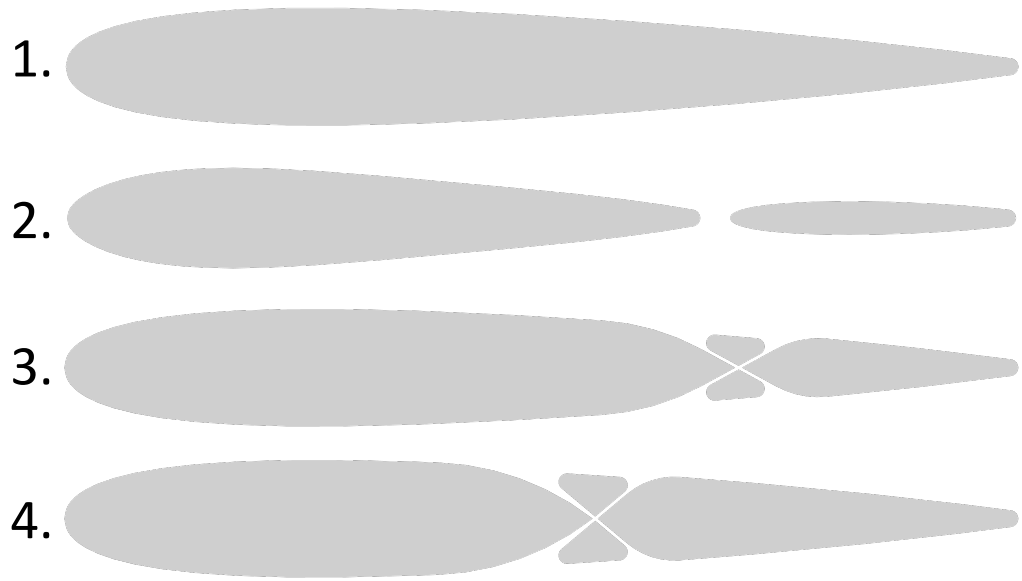

Figure 3.17: Shape of compared airfoils

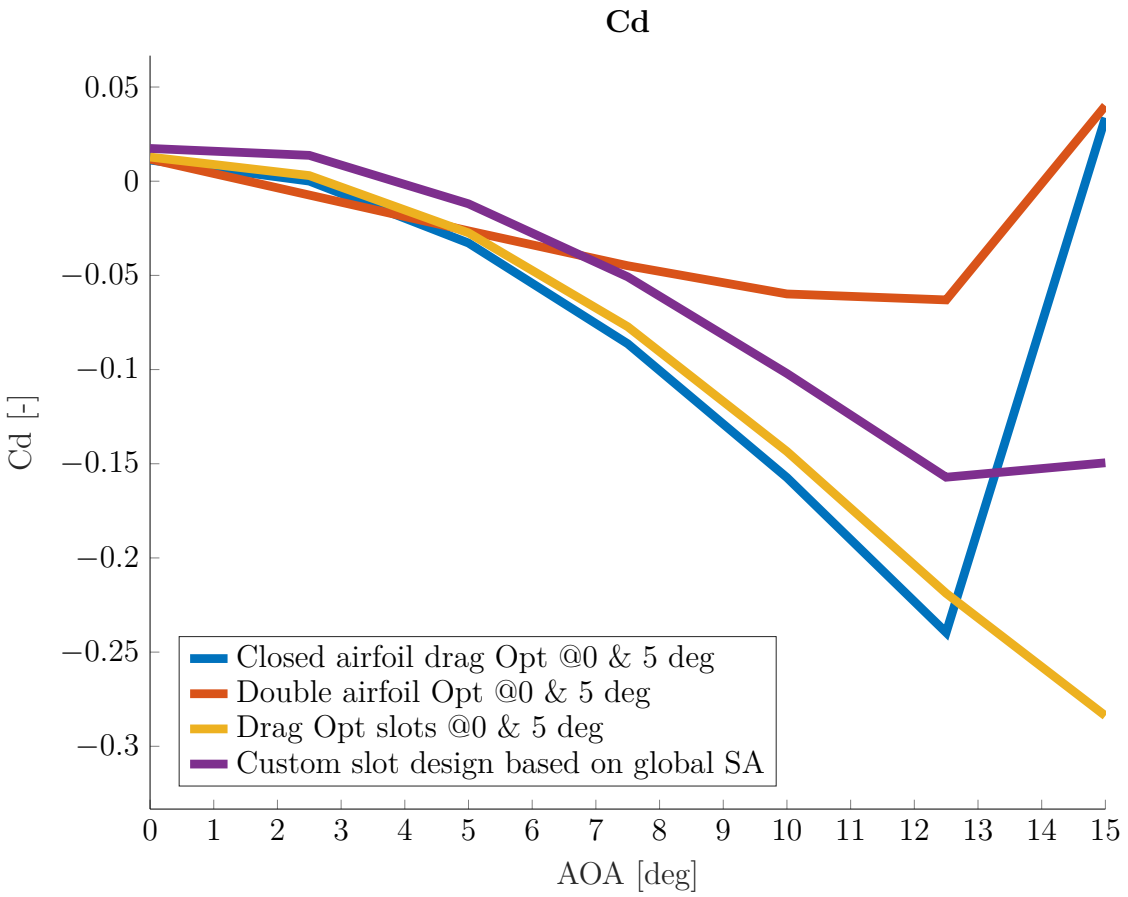

Figure 3.18: Plot of Cd for the final design airfoils

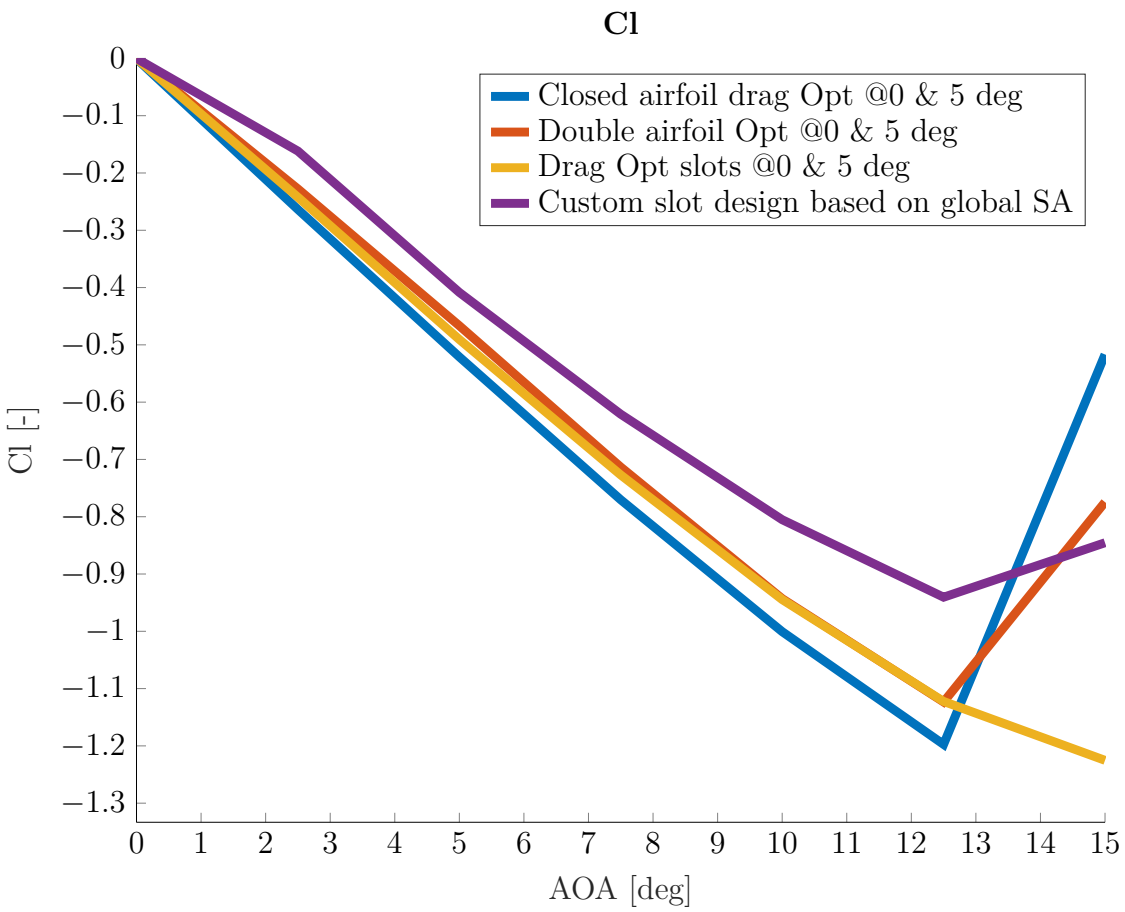

Figure 3.19: Plot of Cl for the final design airfoils

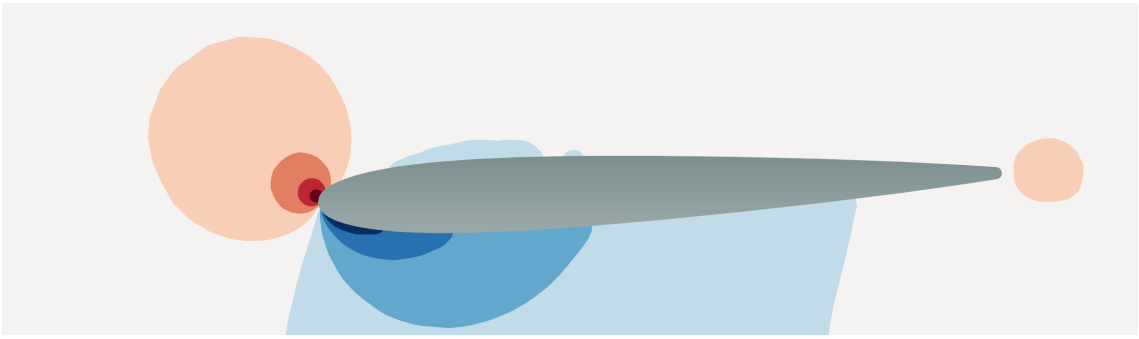

(a) Pressure plot for closed airfoil at 2.5 *deg* of attack angle

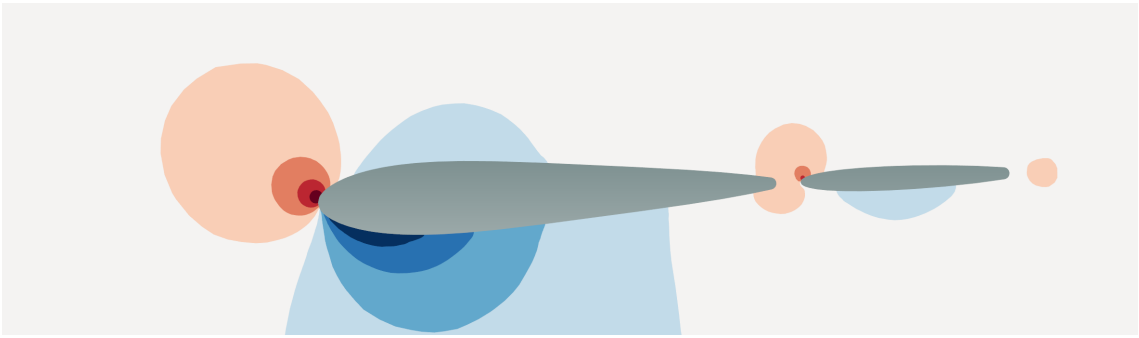

(b) Pressure plot for double airfoil at 2.5 *deg* of attack angle

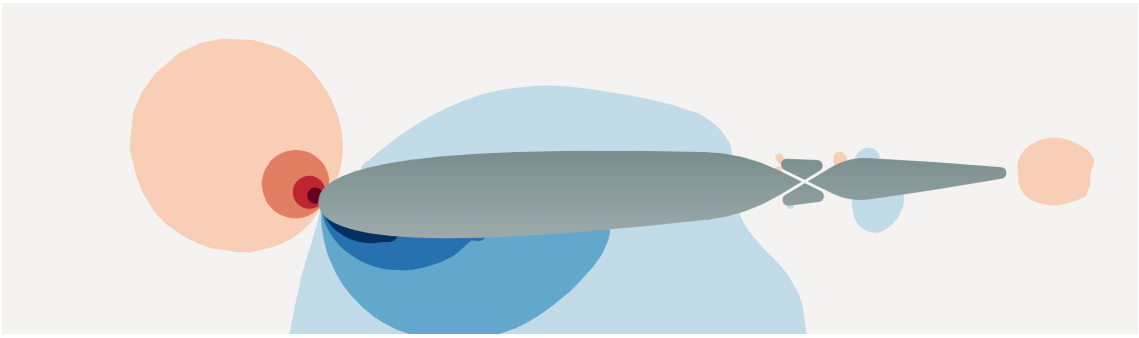

(c) Pressure plot for slotted airfoil at 2.5 *deg* of attack angle

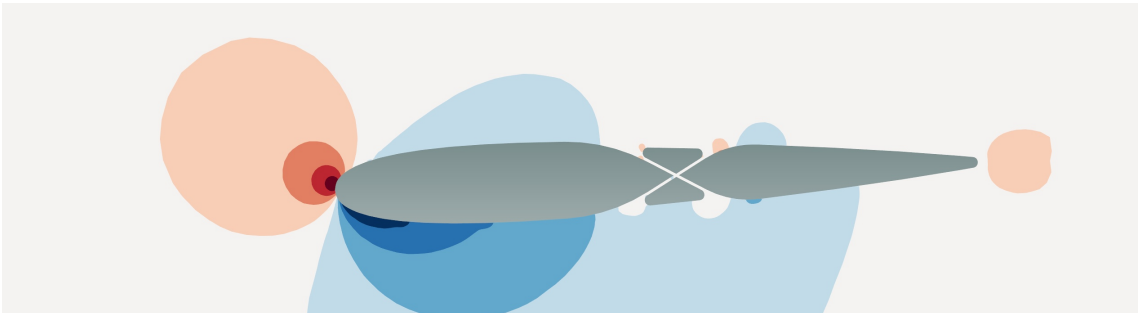

(d) Pressure plot for slotted airfoil designed from SA at 2.5 *deg* of attack angle

Figure 3.20: Pressure plots of all the four airfoils at 2.5 *deg* of attack angle

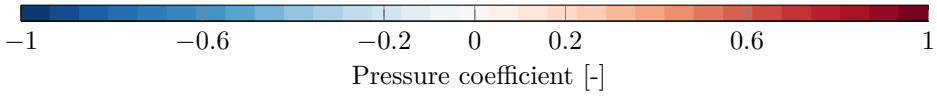

When investigating further why the double airfoil loses performance from 5 *deg* of attack angle and up a possible explanation was found. It is possible to see in figure 3.21a that the flow between the airfoils increases with larger angles of attack, but the drag also increases due to that the stagnation point on the second airfoil increases. When more flow goes through the gap between the airfoils, the flow under the second airfoil accelerates and a lower pressure is achieved, but the amount is not enough to compensate for the increased stagnation pressure at the leading edge.

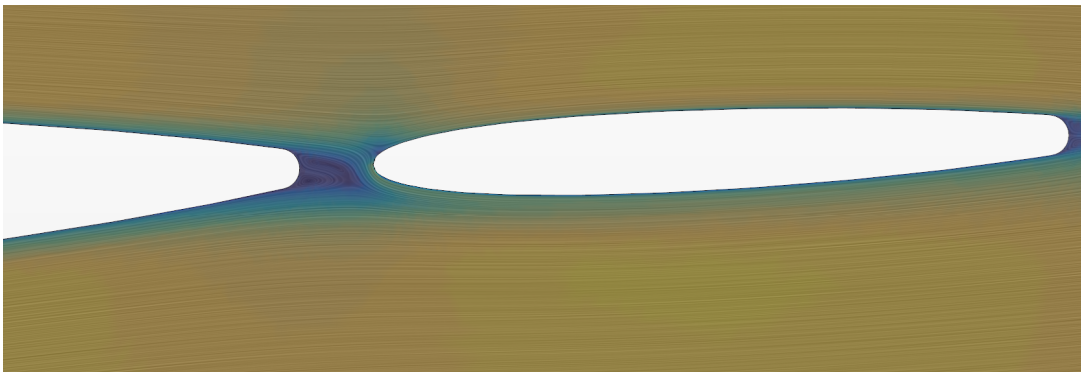

(a) Attack angle of 2.5 *deg*

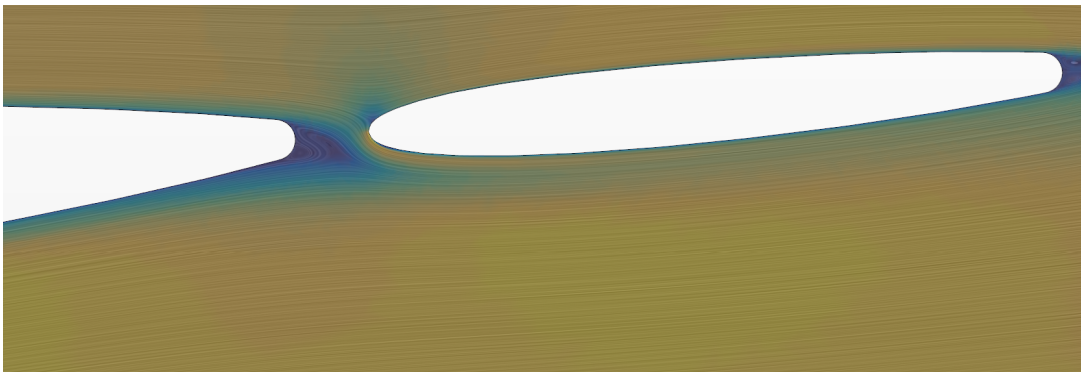

(b) Attack angle of 5 *deg*

Figure 3.21: Flow between the two airfoils at 2.5 *deg* and 5 *deg* of attack angle

3.4 Discussion

In order to improve the airfoils even further and gain more lateral force while cornering, active control of the pylon could be implemented. Making the pylon active opens up new possibilities to explore, where the airfoil can be optimized for different scenarios and then switch between them. With an active pylon, it would be possible to help in both over- and understeer situations since you could control in which direction the lateral force on the pylon would act and thus improving handling. Since the force generated by the pylon will act towards the center of the curve, more load will be added on the inner rear wheel. This will lead to an increased total grip of the

rear axle and by such the vehicle will be more understeered, this is the case when having a passive pylon. This can also be achieved with an active pylon, but the force could also be pointed outwards with the help of an active pylon, that would mean more load on the outer rear tyre which will lead to a more oversteered car while cornering. The double airfoil is especially well suited for the implementation of active control since the rearmost airfoil section could be made to rotate and by such guiding the air while the front airfoil can make sure that the pylon has enough structural strength to cope with the forces from the wing. Two drawbacks of implementing active control on the pylon is a factor of complexity and an increase in weight. The engineering required in order to make a part of the pylon rotate is far more advanced than just having a stationary part and it will also require additional parts in order to work. Since Lamborghini is a sports car manufacturer the added weight can also be something that is unwanted, as that has a negative effect on the vehicle dynamics.

It would have been very interesting to do a sensitivity analysis on the two airfoil sections of the double airfoil and find out which parameters are the most influential on this design. Further analysis of the double airfoil could result in an excellent pylon that, as mention previously, have a large potential of being turned into an active aerodynamic device down the line.

To be able to verify the results from a full vehicle 3D simulation or wind tunnel tests would have to be made. Unless the flow interacts with the entire vehicle up to the point where the pylon is located it is not possible to know exactly how the flow will behave around the pylon. Though it was concluded at the beginning of this project that the flow at the rear of the car will almost certainly have a relatively large Reynolds number and thus the simulations have been run with that in mind.

An interesting aspect that has been discovered during this thesis is that airfoil with the lowest drag and the one with the largest generated lift is often the same one. Since the investigation has been made in the local coordinate system an airfoil with a large lift helps to propel the vehicle forwards when the angle of attack is increasing, the outcome of this is a decreasing drag, this is similar to a sailing boat or a wind turbine. 0 deg of attack angle is the one area where the lift and drag does not correspond, as should be expected.

4 Conclusion

By designing a pylon with handling properties in mind it is possible to create a lateral force that could be utilized while cornering. A pylon that creates a large lateral force also helps to propel the vehicle forwards when the attack angle of the wind is larger than 0 *deg*.

With both the slotted design and the double airfoil there is potential of creating airfoils that have good drag performance while still generating a lateral force.

Passive control of an airfoil can lead to better performance, though the location of where the passive control is located is of most importance for it to be efficient. What has been found is that if you put the passive solutions too close to the front of the airfoil, it will most likely have a negative effect on performance. The balance that is hard to find is that the passive control should be located far enough from the front to not affect the flow at low angles of attack, but at the same time not too far towards the rear where the passive control will lose its efficiency. There is by such no definitive measure that is the best, a lot of factors such as the airfoil shape and the type of passive control used affect where in the streamwise direction the solution should be implemented.

It is not possible to know if the designs created can help with the reduction of the 3D-separated area at the contact between the pylon and the rear wing. The possible benefit from the reduction of the 3D-separated area is therefore not quantified, further analysis in the matter is required.

There is a reason that the NACA airfoils have been used for as long as they have, they are really good airfoils. Even though the closed airfoil that was created during this thesis was slightly better in some regards such as how much attack angle it could handle before the flow became separated, in the end the NACA profile performed similarly in the focus range of 0 *deg* to 5 *deg* to the created airfoil it was compared to. When designing a new symmetrical airfoil shape, the NACA profiles are good starting points that can be tweaked to improve performance at higher angles of attack without large influence at lower angles of attack.

References

Abbott, I. H., & Doenhoff., A. E. (1959). *Theory of wing sections.* Dover Publications, inc., New York.

AirfoilTools. (2020). *Airfoil generator.* Retrieved from `http://airfoiltools.com/`

Galan, C. (2020). *Airfoil generator, matlab central file exchange.* Retrieved from `https://www.mathworks.com/matlabcentral/fileexchange/54677-airfoil-generator`

Jeff Bezanson, S. K. V. B. S., Alan Edelman. (2017). *Julia: A fresh approach to numerical computing.* Retrieved from `https://julialang.org/research/julia-fresh-approach-BEKS.pdf`

Katz, J. (2006). *Race car aerodynamics: Designing for speed.* Bentley Publishers, Massachusetts.

Magnus Urquhart, S. S., Emil Ljungskog. (2020). *Surrogate-based optimisation using adaptively scaled radial basis functions.* Retrieved from `https://www.sciencedirect.com/science/article/pii/S1568494619308324`

McBeath, S. (2015). *Competition car aerodynamics.* Veloce Publishing Limited, Dorchester.

Timmer, W. A. (2010). Aerodynamic characteristics of wind turbine blade airfoils at high angles-of-attack..